4.2 SUMMARY OF RESULTS FOR CAI #2

RADGUNS should accurately simulate weapon system tracking performance during all types of engagements. This assessment aims to validate model performance against non-maneuvering targets of varying sizes at various speeds in a dry (non-ECM) environment. Because the antenna servo outputs are inputs to the fire-control computer, tracking performance directly affects shooting performance and overall system effectiveness.

In *RADGUNS* v.1.8, assessment of angle and range track at the functional level revealed differences between the available intelligence estimates of servo transient response and modeled transient response. During this assessment, the servo transfer function coefficients were modified, resulting in improved correlation at the FE level. Tracking performance was also assessed at the model level by comparing tracking errors produced by both *RADGUNS* v.1.8 and v.1.8 with the modified transfer function coefficients to measured system errors. Performance at this level was target dependent. Model correlation with B-1B data was greatly improved when the servo coefficients where adjusted in *RADGUNS*. With the modified transfer functions, the model closely predicted the mean, standard deviation, and range of azimuth and elevation errors (with system biases removed). Version 1.8 produced range errors with a much larger bias, standard deviation, and range than exhibited by the system. Although the modified transfer functions greatly reduced these, discrepancies still existed in the range channel. Inconsistencies in the T-38 elevation data excluded it from the analysis. In azimuth and range, however, *RADGUNS* v.1.8 predicted the standard deviation and range of errors better than the modified version, and when biases were removed, correlation with test data was very good. In comparisons with F-15 data, *RADGUNS* v.1.8 approximated the frequency content of the tracking errors better than modified version, and again correlation with test data was good. In all cases examined, the mean angular errors generated by the model differed from those measured from the system by a maximum of 13 meters at the range of the target. Errors of this magnitude, when translated to angles at the threat, may be limited by the accuracy of the instrumentation used to collect the data. Mean range errors differed by a maximum of 15 meters (6 m with the modified coefficients) for the large target, and within 4 meters for the smaller targets. Again, the data may be limited by the accuracy that can be achieved on the range. These three data sets were again used to assess tracking performance in *RADGUNS* v.1.9. An additional data set was analyzed. This data is described below.

Test Data Description. Four flight tests were conducted at two test ranges. Data collected from three threat systems during these tests were used to assess tracking performance. A well designed track loop should maintain errors with a small standard deviation about zero. Thus, mean, standard deviation, and the range of errors were used as MOEs in this assessment. Tracking error time histories where also analyzed for general trends. Table 4.2-1 summarizes the results of this assessment.

TABLE 4.2-1. Target Tracking Assessment Summary.

Test/Target	Major Conditions	Statistical MOE	Results
Giant Hawk/B-1B	Straight and level, no ECM	Mean, standard deviation, range of errors	Correlation with angle errors good
CERTS / T-38	Straight and level, no ECM	Mean, standard deviation, range of errors	Correlation with angle errors good

TABLE 4.2-1. Target Tracking Assessment Summary. (Contd.)

Test/Target	Major Conditions	Statistical MOE	Results
CERTS / F-16	Straight and level, no ECM	Mean, standard deviation, range of errors	Correlation with angle errors good
WEST XI / F-15	Straight and level, no ECM	Mean, standard deviation, range of errors	Correlation with angle and range errors good

Validation Methodology. Portions of straight and level passes were selected where the radar was in full autotrack mode and the MTI switch was in the "OFF" position. The reference tracker's x, y, and z positions were used to generate BLUMAX flight paths for input to the model. The model was executed with the following conditions:

Model mode:	SINGL/RADAR
Radar type:	RAD1
Target type:	B-1B / T-38 / F-16 / F-15
Flight path:	BLUMAX
MTI mode:	OFF
Clutter/Multipath:	None
Outputs (10 Hz):	Tracking error, presented dimensions of target in horizontal and vertical directions

Preliminary comparisons between measured and model data revealed that the model tracked much better than the system. Modeled errors were consistently close to zero with a very small range of values. Because validation of angle and range track at the functional level showed good correlation between modeled servo transient response plots and intelligence estimates, it was concluded that either the system was unnecessarily noisy or some input to the target tracker was improperly modeled in *RADGUNS*. Assessments of the AGC response showed good correlation between measured and model data. In an effort to introduce noise in the modeled system where it might actually occur in the real system, the target signature was varied randomly within *RADGUNS* uses a static RCS target model, when, in fact, actual target signatures fluctuate widely about a static value. In general, adding target fluctuations improved the overall correlation with data.

In *RADGUNS*, tracking errors are the difference between the perceived target position and the position of the target centroid. On the range, however, tracking errors are calculated as the difference between two perceived — threat radar's tracked position and the reference tracker's position. Both radars are susceptible to glint effects and, in some instances, one radar may be tracking the nose of the aircraft, or worse, half a beamwidth off the front of the nose while the other tracks the tail. In an effort to minimize the propagation of TSPI errors into computed tracking errors, the following procedure was used.

Targets are modeled in *RADGUNS* as ellipsoidal areas. The ratio of the major axis to the minor axis changes as the target aspect angle changes and is determined by the presented

area of the target and the target wingspan, body height, and length. In most instances, this ratio is close to 4. The model computes the radius in the horizontal and vertical directions based on the aspect angle of the target at any given point in the flight path. For both the reference and threat radars to be tracking at some point on the target, the magnitude of the azimuth error in meters at the range of the target can be no larger than the presented length in the horizontal direction, while the magnitude of the elevation error can be no larger than the presented height in the vertical direction (see Figure 4.2-1).

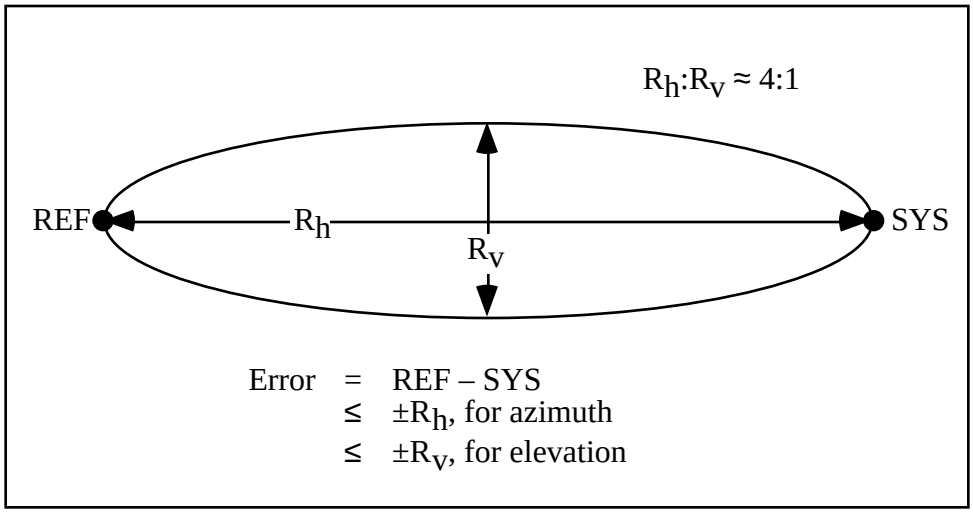

FIGURE 4.2-1. Data Selection Criterion.

Thus when the error exceeds the presented dimensions of the target in either the horizontal or vertical direction, at least one of the tracker boresights is not on the target, and it is impossible to determine which system's performance is being degraded. It is unreasonable to expect the model to predict the measured performance of the system when these error bounds are exceeded. For each of the passes examined, the presented target dimensions are superimposed on the azimuth and elevation error time histories to determine areas where model performance should be analyzed. Range error should ideally be no larger than the largest dimension of the target in the radial direction from the threat. This value is not readily accessible in the model, so the largest target dimension, length, was used as a rough estimate of range bounds.

Each engagement is identified by an eight-digit designator and a two-digit run number (e.g., R01). The first three digits name the target, the fourth and fifth describe the threat, and the last three digits contain the day in the year that the test was conducted.

4.2.1 Assessment – Case 1

Assessment Description – B-1B

Test Data Description. The tracking performance of one AAA threat system against a single B-1B target was measured in a dry environment during the Giant Hawk FOT&E. The aircraft flew relatively straight and level profiles at various offsets from the threat system at approximately 277 m/s.

Validation Methodology. Two trackers were used to provide TSPI reference data. When possible, the reference tracked a beacon located on the top of the fuselage near the center of the aircraft. Prior to the start of each mission, the trackers toggled between skin and beacon track to establish a beacon delay time. Data from both trackers, the beacon delay time, and other "historical tracker information" were used as inputs to a TSPI smoothing algorithm. TSPI was then translated and rotated to the threat location via post-test processing.

Measured tracking errors were obtained by subtracting the aircraft position, as perceived by the threat, from the position perceived by the reference. Range personnel estimated the reference position to be accurate to within in beacon track mode. When relying on a skin return, however, glint effects may cause the reference to wander about the extent of the aircraft.

Data were collected at ten samples per second. Aircraft and reference tracker data were time-correlated to the threat data using interpolation where necessary. Table 4.2-2 shows the data fields available for this analysis (see the Test Summary Report for Existing *RADGUNS* Data for a detailed description of each field).

TABLE 4.2-2. B-1B Data Fields.

Field	Description
DELTA_AZ DELTA_EL DELTA_RG	Azimuth, elevation, and range tracking errors; the result of mathematically subtracting the reference TSPI position from the threat's perceived position
REF_X_POS REF_Y_POS REF_Z_POS	TSPI tracker's aircraft position rotated to the threat's location, where positive *x* is east, positive *y* is north, and positive *z* is up
REF_XVEL REF_YVEL REF_ZVEL	X-, Y-, and Z-components of aircraft velocity rotated to the threat's location
MTAZ_0 MTEL_0 MTRG_0	Threat's azimuth, elevation, and range tracking modes
RTMTI_ON1	MTI mode (ON/OFF)

Segments were selected from three passes where the radar was in full autotrack mode and the MTI switch was off. Table 4.2-3 lists the direction of aircraft travel, the offset from the threat, the direction of offset, and the average altitude and speed of the aircraft.

TABLE 4.2-3. B-1B Test Matrix.

System	Pass	Type	Direction	Offset (m)	Offset Direction	Altitude (m)	Speed (m/s)
2	2	LINEAR	SE/NW	734	SW	223	277
2	13	LINEAR	NW/SE	33	NW	571	281
2	14	LINEAR	SE/NW	904	SW	499	274

Figures 4.2-2 through 4.2-4 show the system tracking error time histories for each of the three runs examined with the horizontal dimension of the target superimposed on the azimuth error plot and the vertical dimension superimposed on the elevation plot. The scale on the range error plot is approximately equal to the length of the target.

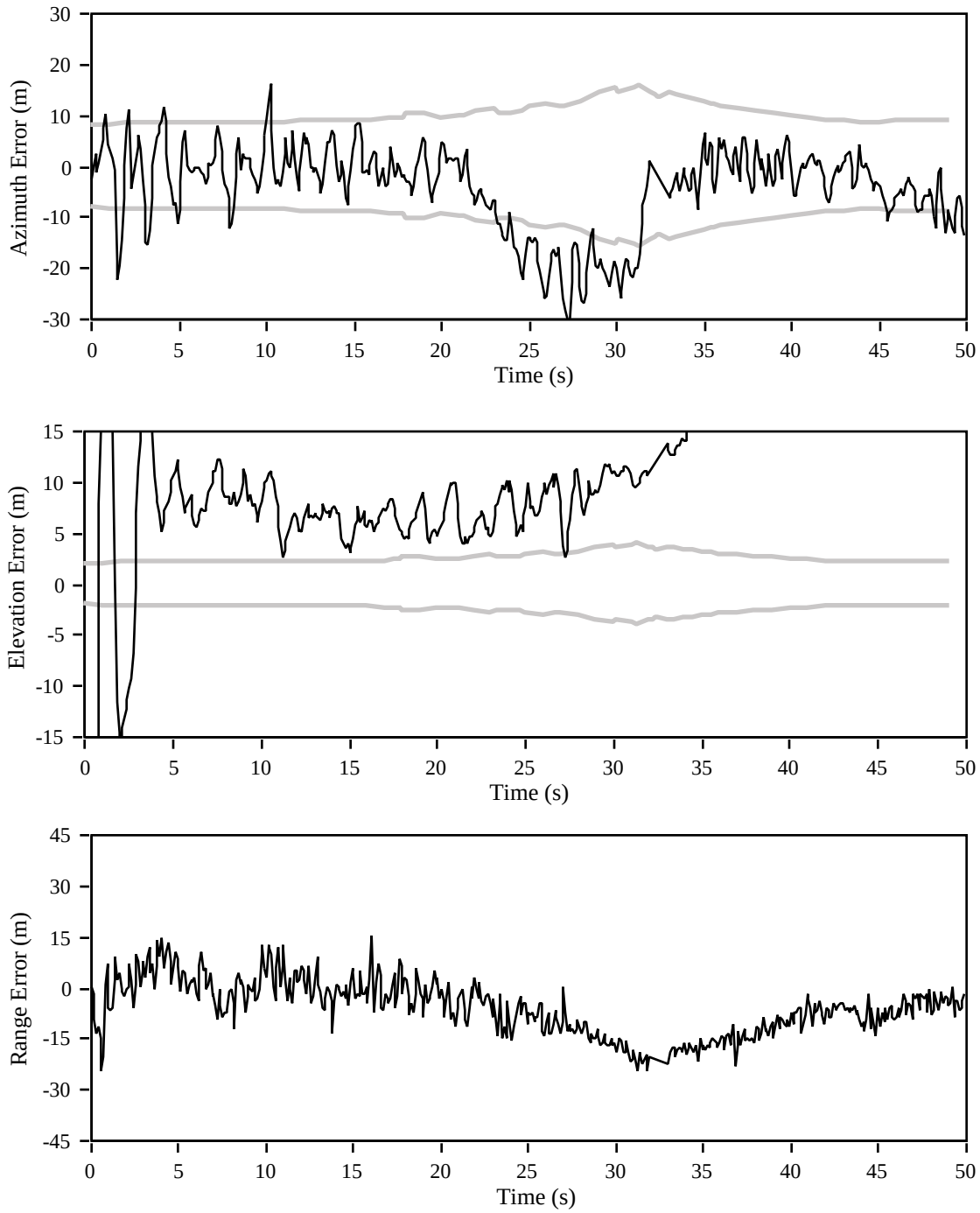

FIGURE 4.2-2. B1B02274 R02 (System Tracking Errors.

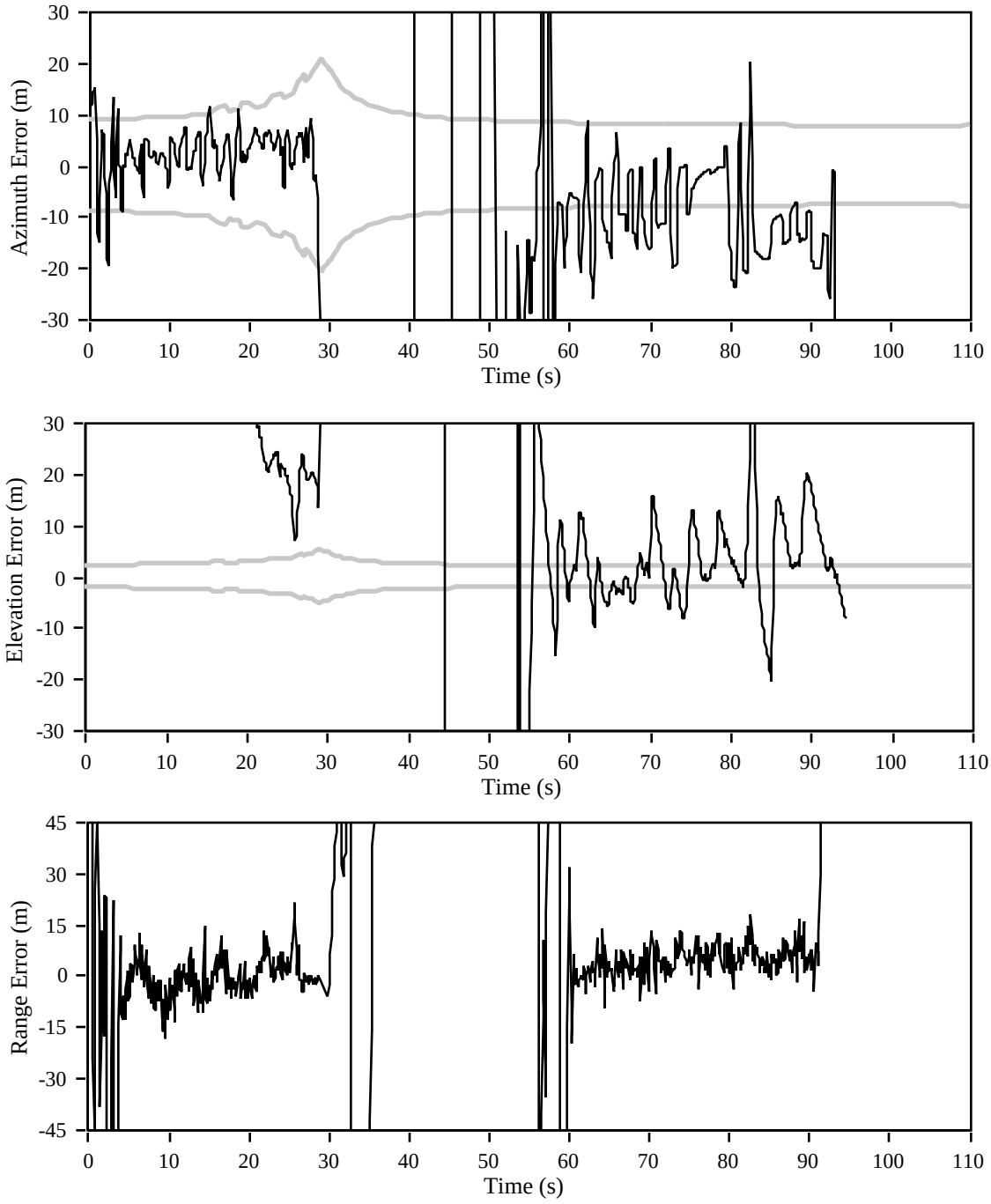

FIGURE 4.2-3. B1B02274 R13 (System Tracking Errors.

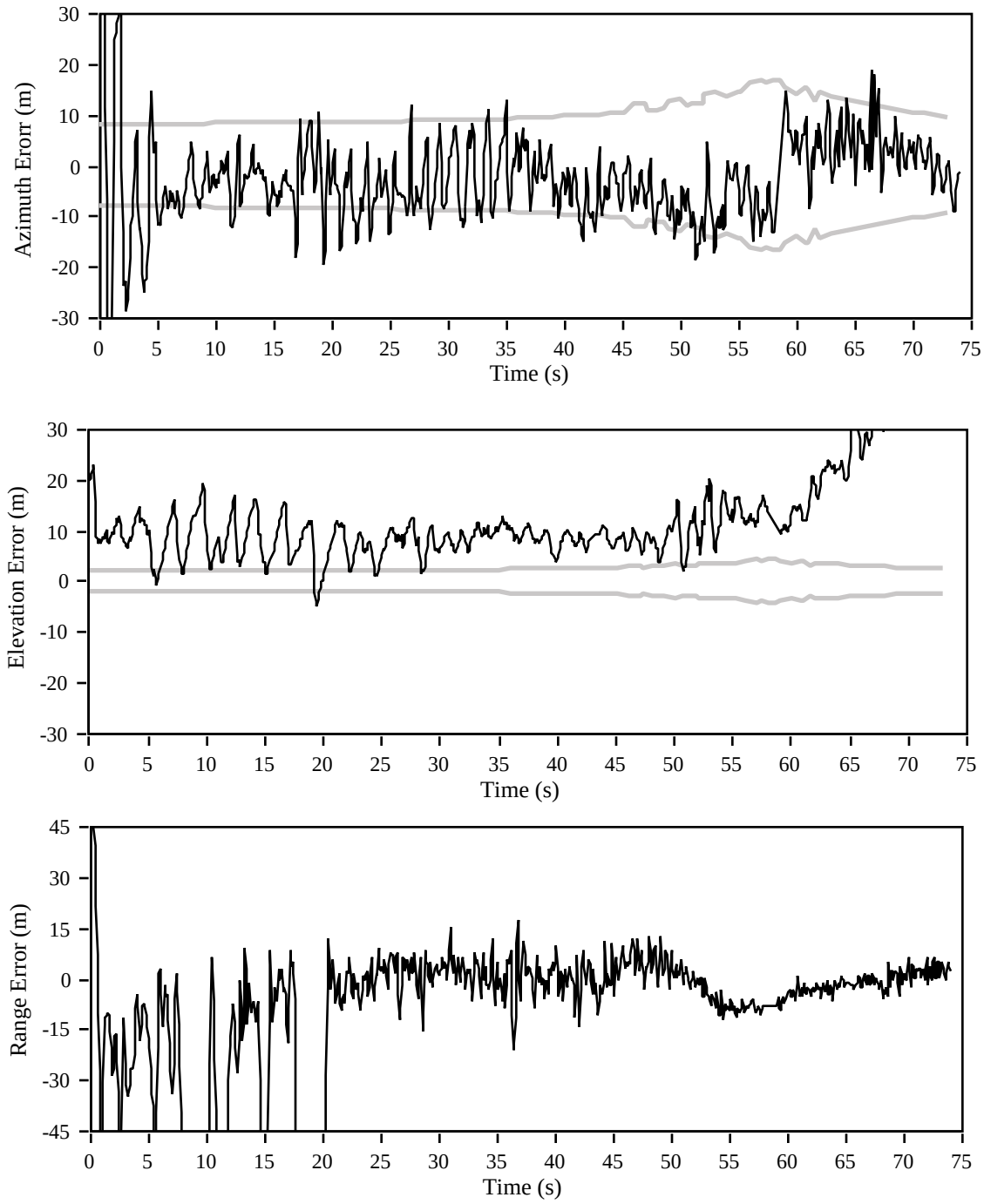

FIGURE 4.2-4. B1B02274 R14 (System Tracking Errors.

The errors are reasonably close to the azimuth bounds from 5 to 20 s during run 2, from 4 to 27 s during run 13, from 35 to 51 s, and again from 67 to 76 s during run 14. The elevation errors do not fall within the bounds for any significant amount of time during any of the passes. At long ranges (i.e., at the start of each run), some elevation error may be attributed to multipath; however, at closer ranges where the elevation angle exceeds a few

degrees, this effect is minimized. In each case, the system develops a constant elevation bias of approximately 10 mrad when the aircraft is flying northwest of the threat. The threats are periodically measured for levelness. The resulting "leveling" factor is used in post-processing calculations. Range personnel suggested that an incorrect factor might produce a constant bias in elevation in a particular sector around the threat. In any case, the model should not be expected to produce constant bias errors. Instead, the model should produce errors similar in frequency and magnitude to those measured from the system when system biases are removed.

Results - B-1B

Appendix A shows tracking errors measured from the system (labeled System), produced by *RADGUNS* v.1.9 (labeled RG1.9), and produced by *RADGUNS* v.1.9 with a fluctuating RCS (labeled RG1.9 fluct). Angle errors are shown in both mrad and m. Figures 4.2-5 through 4.2-8 show tracking errors for the portions of passes 2, 13, and 14 where the azimuth errors fit within the horizontal bounds of the target (as described above). Following the figures are tables containing the mean ($\bar{x}$), standard deviation (s), range (RG), and average of magnitude ($\overline{|x|}$) of errors for each segment. Shaded blocks indicate whether *RADGUNS* v.1.9 with or without target fluctuations best represents the measured MOE.

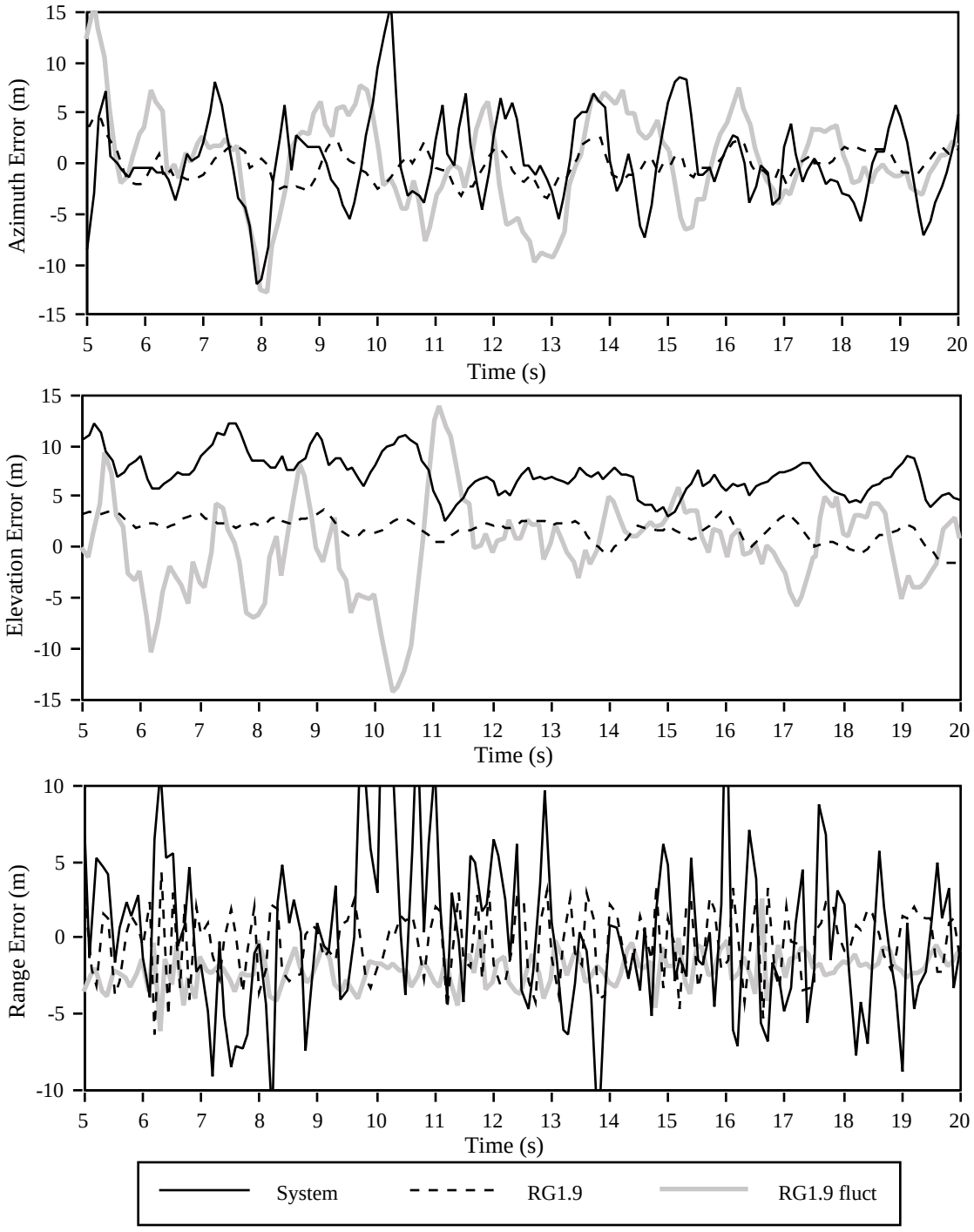

FIGURE 4.2-5. Tracking Errors - B1B02274 R02 (5-20 s).

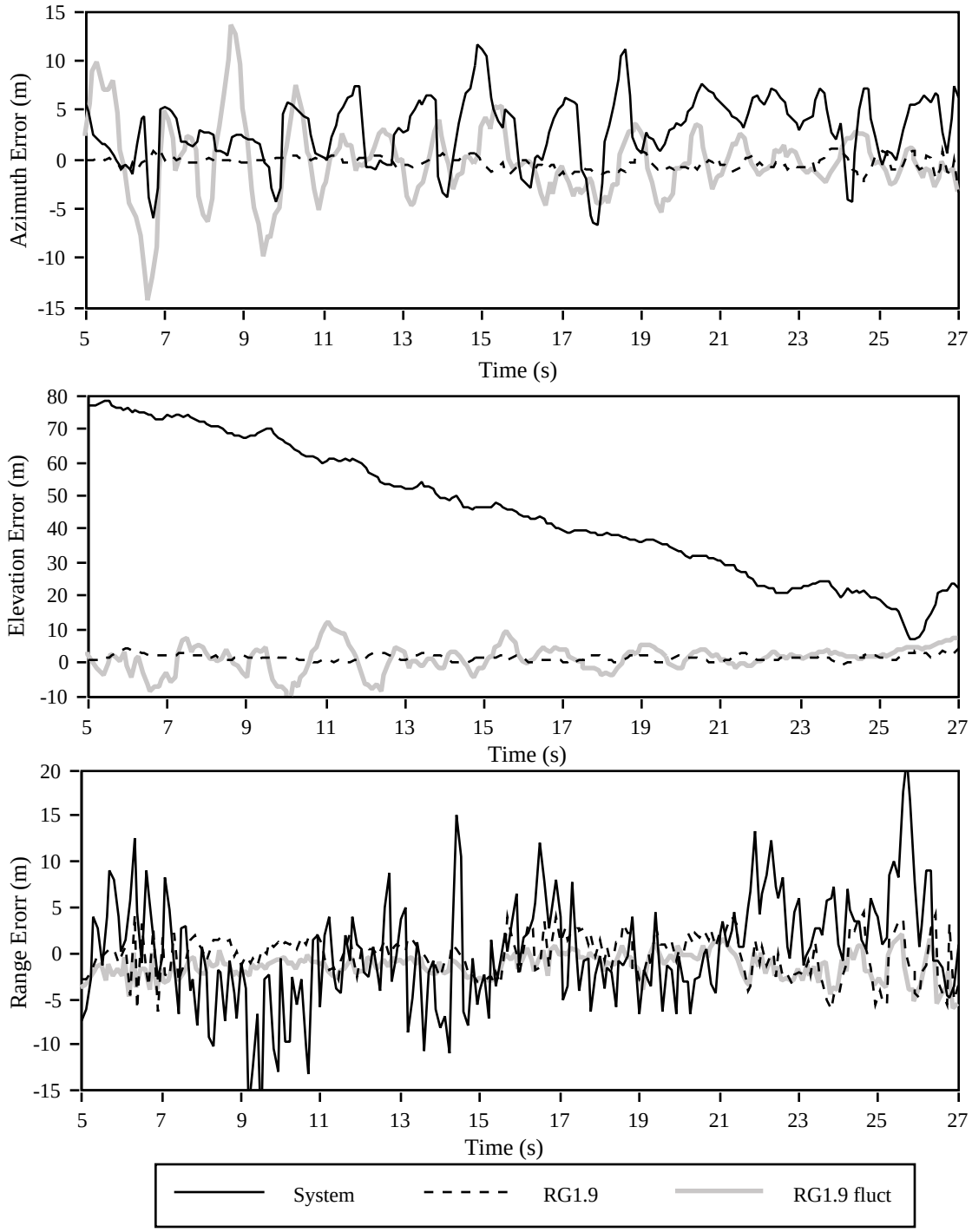

FIGURE 4.2-6. Tracking Errors - B1B02274 R13 (5-27 s).

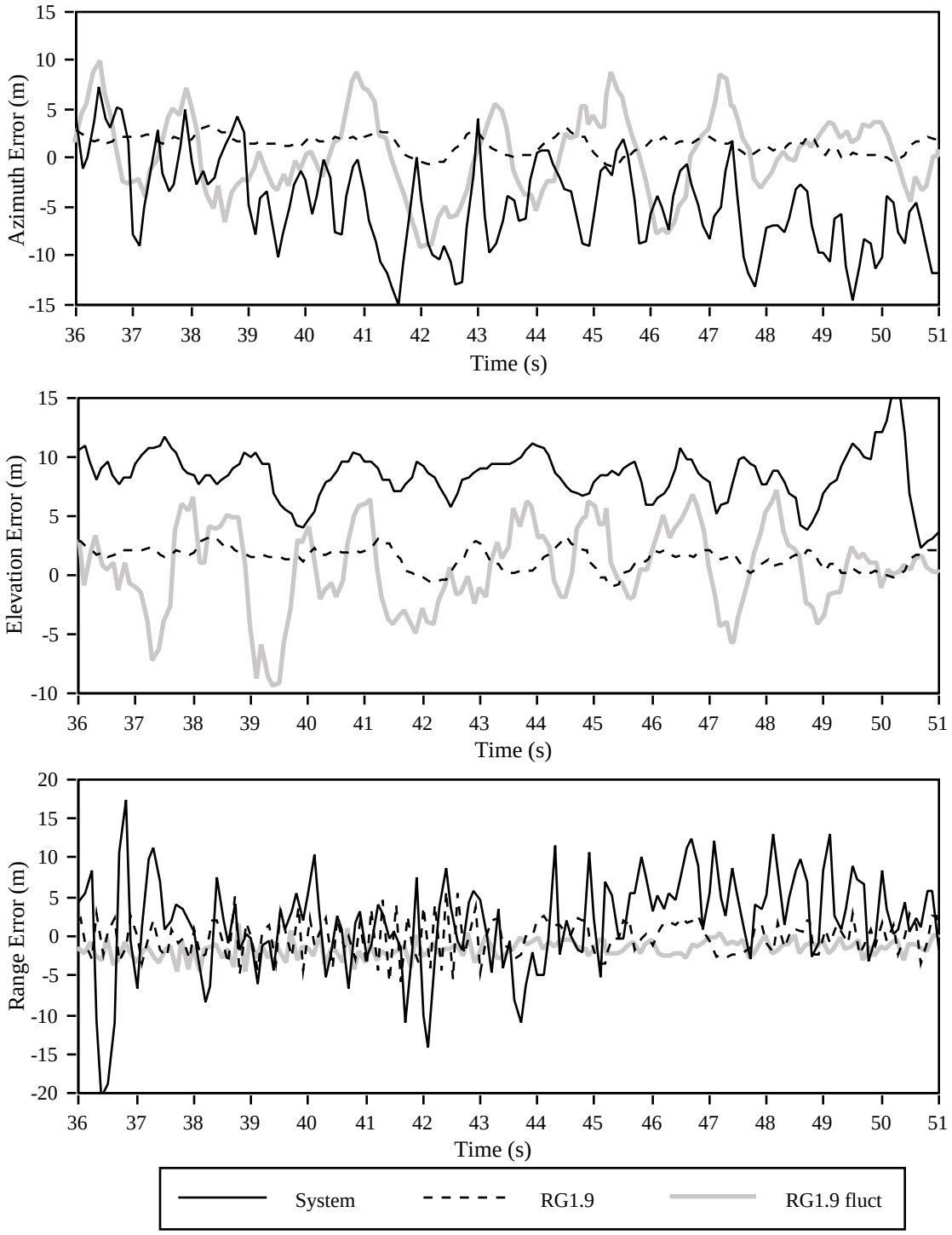

FIGURE 4.2-7. Tracking Errors - B1B02274 R14 (36-51 s).

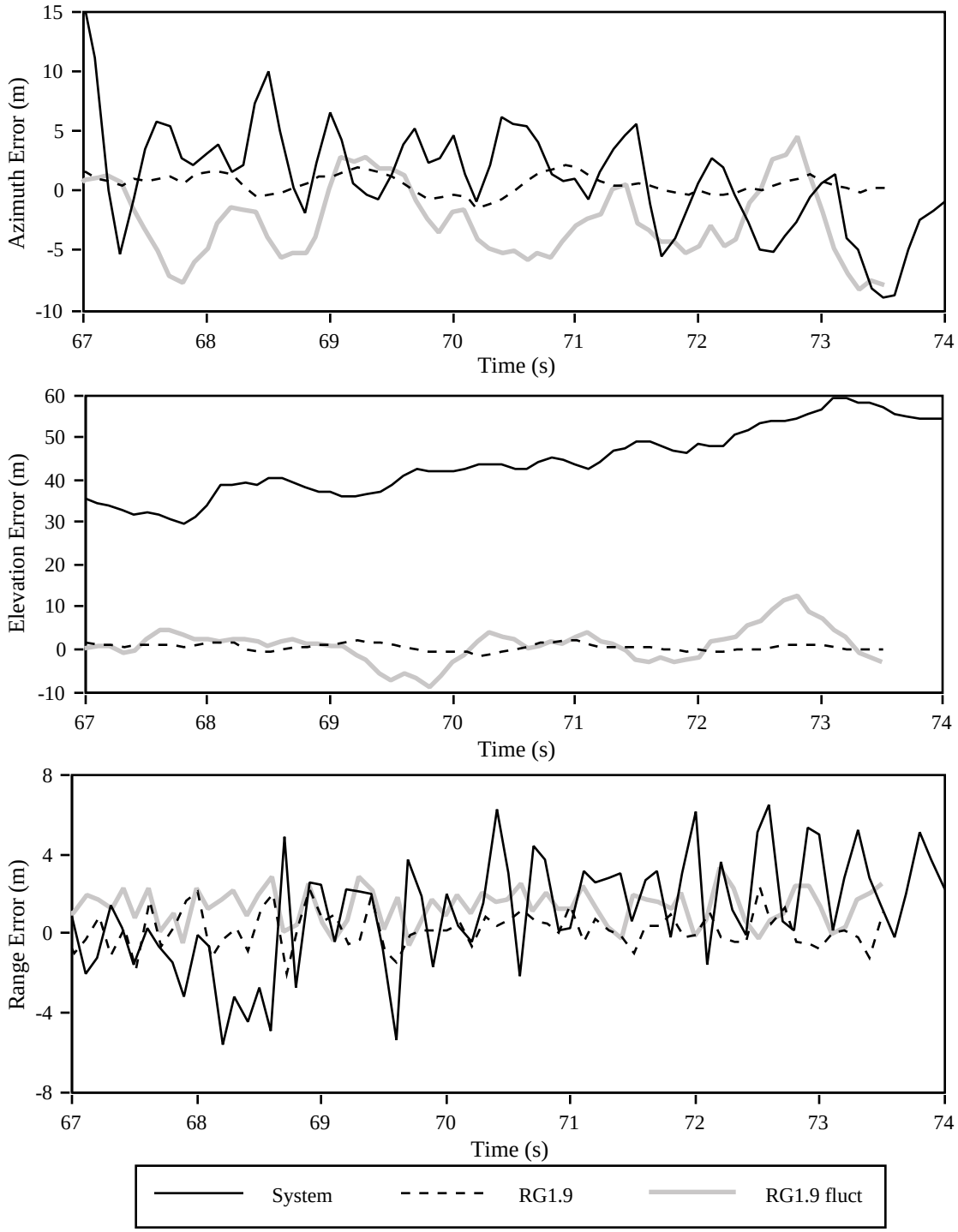

FIGURE 4.2-8. Tracking Errors - B1B02274 R14 (67-74 s).

TABLE 4.2-4. Tracking Statistics - B1B02274 R02 (5-20 s).

MOE	Azimuth Error (m)			Elevation Error (m)			Range Error (m)		
	SYS	RG1.9	RG1.9 fluct	SYS	RG1.9	RG1.9 fluct	SYS	RG1.9	RG1.9 fluct
$\bar{x}$	0.31	-0.12	0.26	8.44	1.37	0.39	1.86	-0.17	-1.77
σ	4.31	1.54	4.88	2.17	0.94	3.66	6.08	2.49	1.16
RG	28.20	7.94	28.68	14.22	4.29	16.57	38.1	11.63	6.02
$\overline{\lvert x \rvert}$	3.26	1.27	3.82	8.44	1.44	3.00	4.95	2.06	1.81

TABLE 4.2-5. Tracking Statistics - B1B02274 R13 (5-27 s).

MOE	Azimuth Error (m)			Elevation Error (m)			Range Error (m)		
	SYS	RG1.9	RG1.9 fluct	SYS	RG1.9	RG1.9 fluct	SYS	RG1.9	RG1.9 fluct
$\bar{x}$	2.92	-0.31	-0.24	45.55	1.46	0.87	0.21	-0.18	-1.51
σ	3.22	0.61	3.82	20.01	0.93	3.91	5.95	2.33	1.40
RG	17.94	2.88	27.79	72.97	4.91	23.15	39.5	10.72	8.21
$\overline{\lvert x \rvert}$	3.65	0.55	2.72	45.55	1.47	3.17	4.55	1.87	1.67

TABLE 4.2-6. Tracking Statistics - B1B02274 R14 (36-51 s).

MOE	Azimuth Error (m)			Elevation Error (m)			Range Error (m)		
	SYS	RG1.9	RG1.9 fluct	SYS	RG1.9	RG1.9 fluct	SYS	RG1.9	RG1.9 fluct
$\bar{x}$	-4.56	0.34	0.19	8.44	1.37	0.39	1.86	-0.17	-1.77
σ	4.73	0.57	4.16	2.17	0.94	3.66	6.08	2.49	1.16
RG	22.31	2.72	18.95	14.22	4.29	16.57	38.1	11.63	6.02
$\overline{\lvert x \rvert}$	5.50	0.54	3.42	8.44	1.44	3.00	4.95	2.06	1.81

TABLE 4.2-7. Tracking Statistics - B1B02274 R14 (67-74 s).

MOE	Azimuth Error (m)			Elevation Error (m)			Range Error (m)		
	SYS	RG1.9	RG1.9 fluct	SYS	RG1.9	RG1.9 fluct	SYS	RG1.9	RG1.9 fluct
$\bar{x}$	2.12	-1.46	-2.82	41.20	0.70	0.88	0.78	0.21	1.26
σ	4.98	0.60	3.05	9.18	0.86	4.00	2.76	1.07	0.90
RG	27.31	3.15	12.56	35.68	3.80	21.33	12.10	5.54	3.88
$\overline{\lvert x \rvert}$	3.96	1.46	3.53	41.20	0.91	3.13	2.28	0.85	1.32

Conclusions - B-1B

RADGUNS v.1.9 produces smaller errors than the system with a smaller standard deviation and range of errors in all cases. Fluctuating the target signature significantly improves correlation in azimuth for each MOE shown in Tables 4.2-4 through 4.2-7. In elevation, adding fluctuations improves correlation with measured range of error and average of magnitude values, however, mean and standard deviation values are improved only some of the time. Range errors produced by *RADGUNS* v.1.9 match measured errors better than *RADGUNS* v.1.9 with a fluctuating target.

Figure 4-9 shows histograms of the tracking errors for run 2. The model represents the system's azimuth distribution much better when the target signature is varied. In elevation, the model produces a one-sided distribution. When fluctuations are introduced, the distribution becomes two-sided, but the spread is much larger than the system's. *RADGUNS* v.1.9 better represents the system's range error distribution.

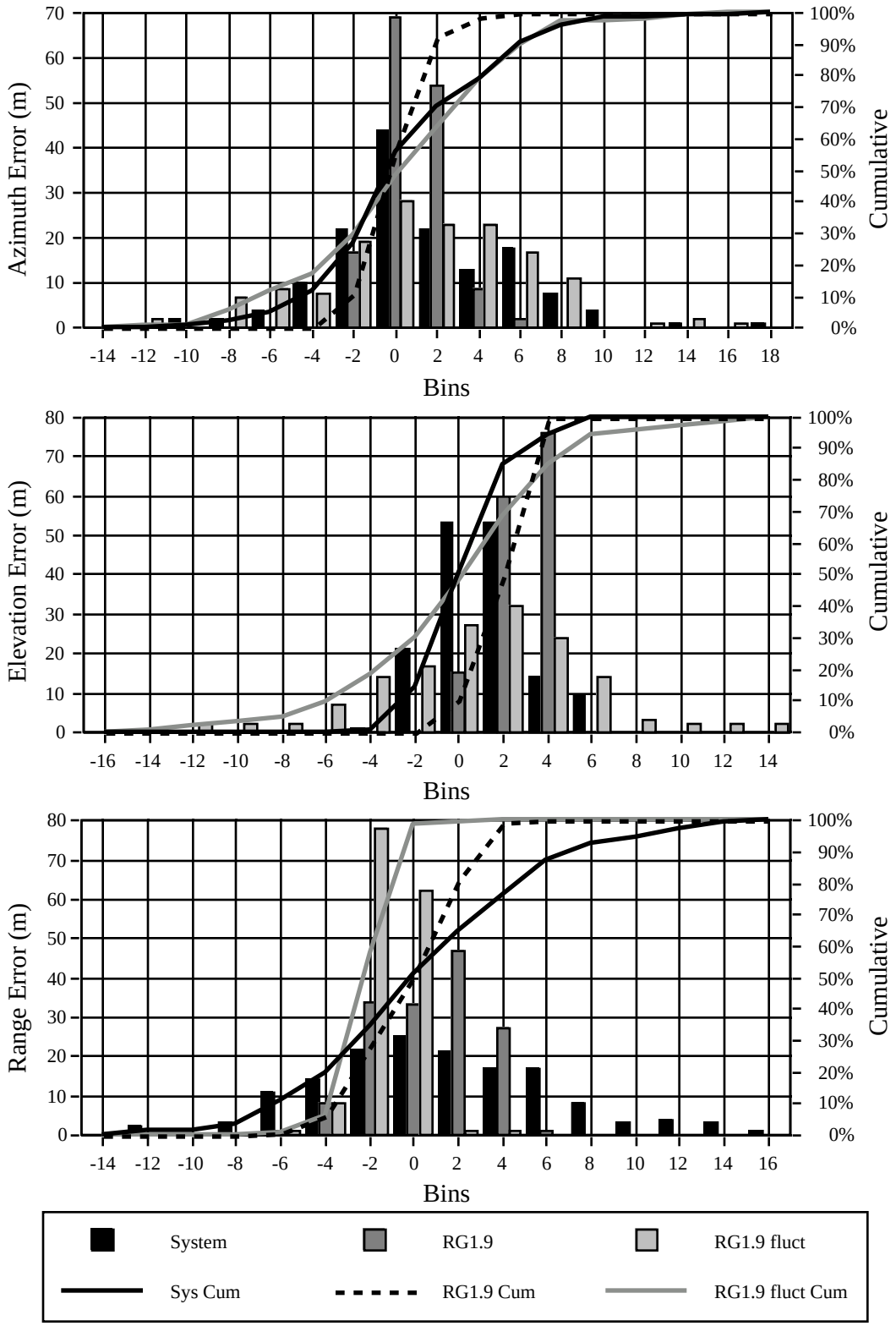

FIGURE 4.2-9. B1B02274 R02 Tracking Error Histograms.

4.2.2 Assessment – Case 2

Assessment Description - T-38

Test Data Description. Tracking data was collected from two AAA threats against a single T-38. This test was conducted on the same range used for B-1B testing, using one of the same threats. The aircraft flew constant altitude, straight and level profiles at various speeds and offsets from the threat systems. The reference trackers used were the same trackers used for the Giant Hawk test, and all data collection and processing techniques used during that test apply here.

Validation Methodology. Visual inspection of tracking error time histories revealed inconsistencies in the data. The two systems produced elevation biases in opposite directions for similar flight paths. Although azimuth trends seemed to be consistent between the two systems, when one is offset in one direction and the other is offset in the opposite direction, there is a sign change in the errors. When looking at a single system, however, offsets in opposite directions did not produce this same effect. In addition, both threat systems developed an unexplained bias in range for the outbound portion of each flight path. Because the T-38 is much smaller than the B-1B, the target dimension criterion used above places much narrower bounds on the data. Table 4.2-8 describes the passes selected for this analysis.

TABLE 4.2-8. T-38 Test Matrix.

System	Run	Direction (from/to)	Offset (m)	Offset Direction	Altitude (m)	Speed (m/s)
4	4	NW/SE	523	NE	478	196
4	7	SE/NW	471	SW	495	183

Flight paths and tracking error time histories are presented in Appendix A. Again, each engagement is labeled with an eight-digit target/threat/date designator and a two-digit run number.

Figures 4.2-10 and 4.2-11 show the system tracking error time histories for the two runs with the horizontal dimension of the target superimposed on the azimuth error plot and the vertical dimension superimposed on the elevation plot. The scale on the range error plot is approximately the length of the aircraft. The azimuth errors are reasonably bounded from 6 to 18 s during run 4 and from 5 to 13 s during run 7. The elevation errors do not fall within the bounds for any significant amount of time.

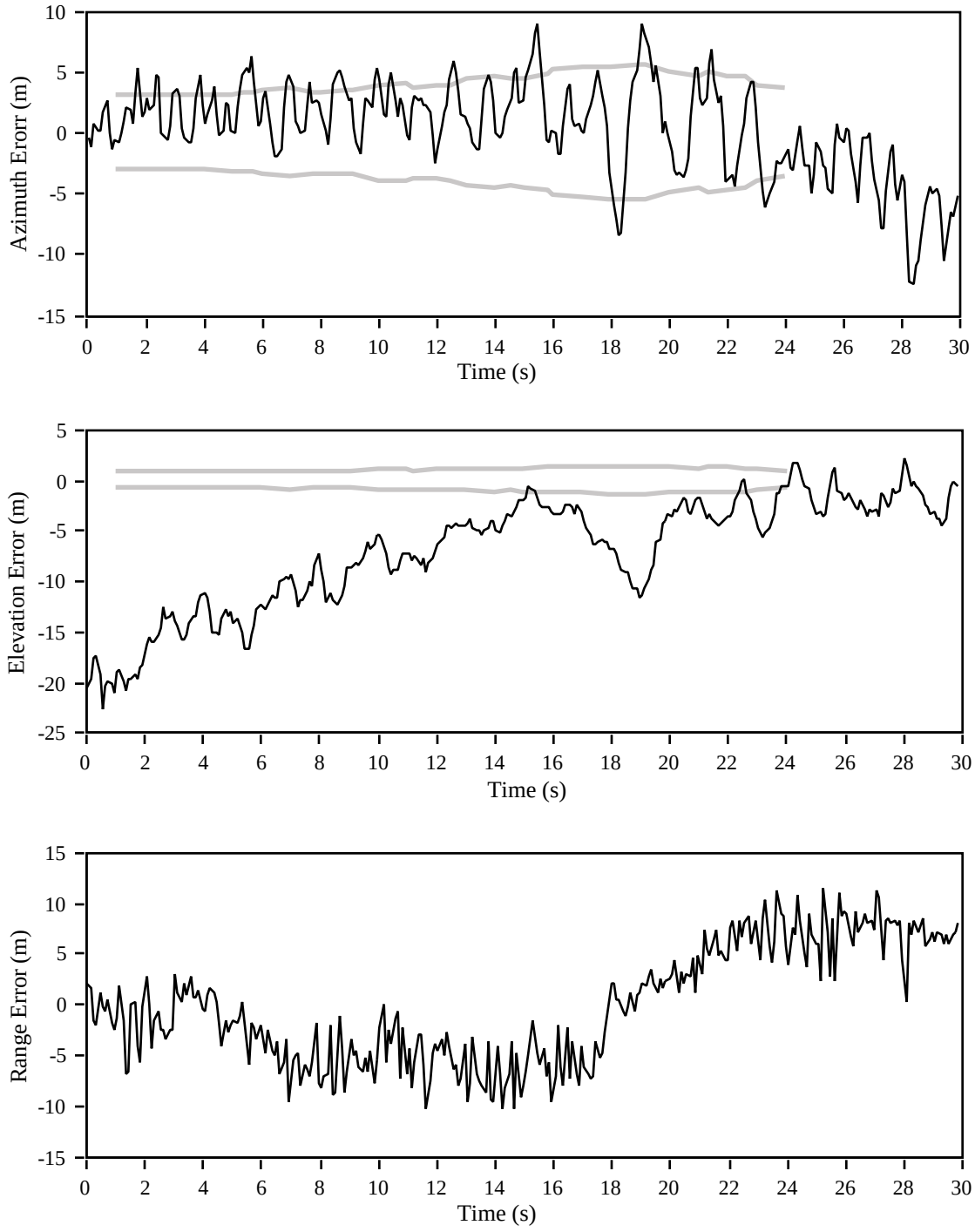

FIGURE 4.2-10. T3804146 R04 (System Tracking Errors).

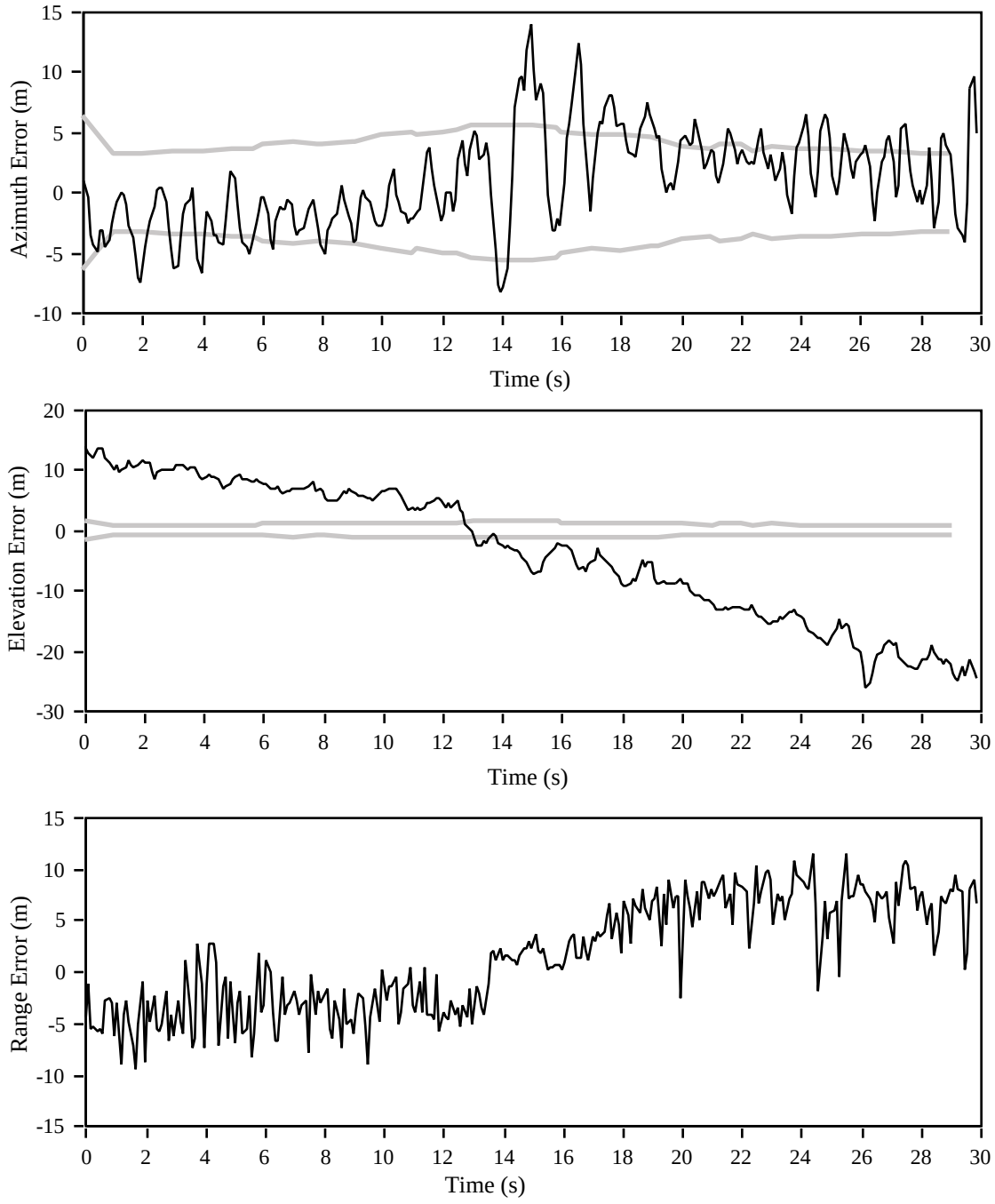

FIGURE 4.2-11. T3804146 R07 (System Tracking Errors).

Results - T-38

Appendix A shows tracking errors measured from the system (labeled System), produced by *RADGUNS* v.1.9 (labeled RG1.9), and produced by *RADGUNS* v.1.9 with a fluctuating RCS (labeled RG1.9 fluct). Angle errors are shown in both mrad and m. Figures 4.2-12 and 4.2-13 show tracking errors for the portions of passes 4 and 7 where the azimuth errors

fit within the horizontal bounds of the target as described above. Following the figures are tables containing the mean ($\bar{x}$), standard deviation (s), range (RG), and average of magnitude ($\overline{|x|}$) of errors for each segment. Shaded blocks indicate if *RADGUNS* v.1.9 with or without target fluctuations best represents the measured MOE.

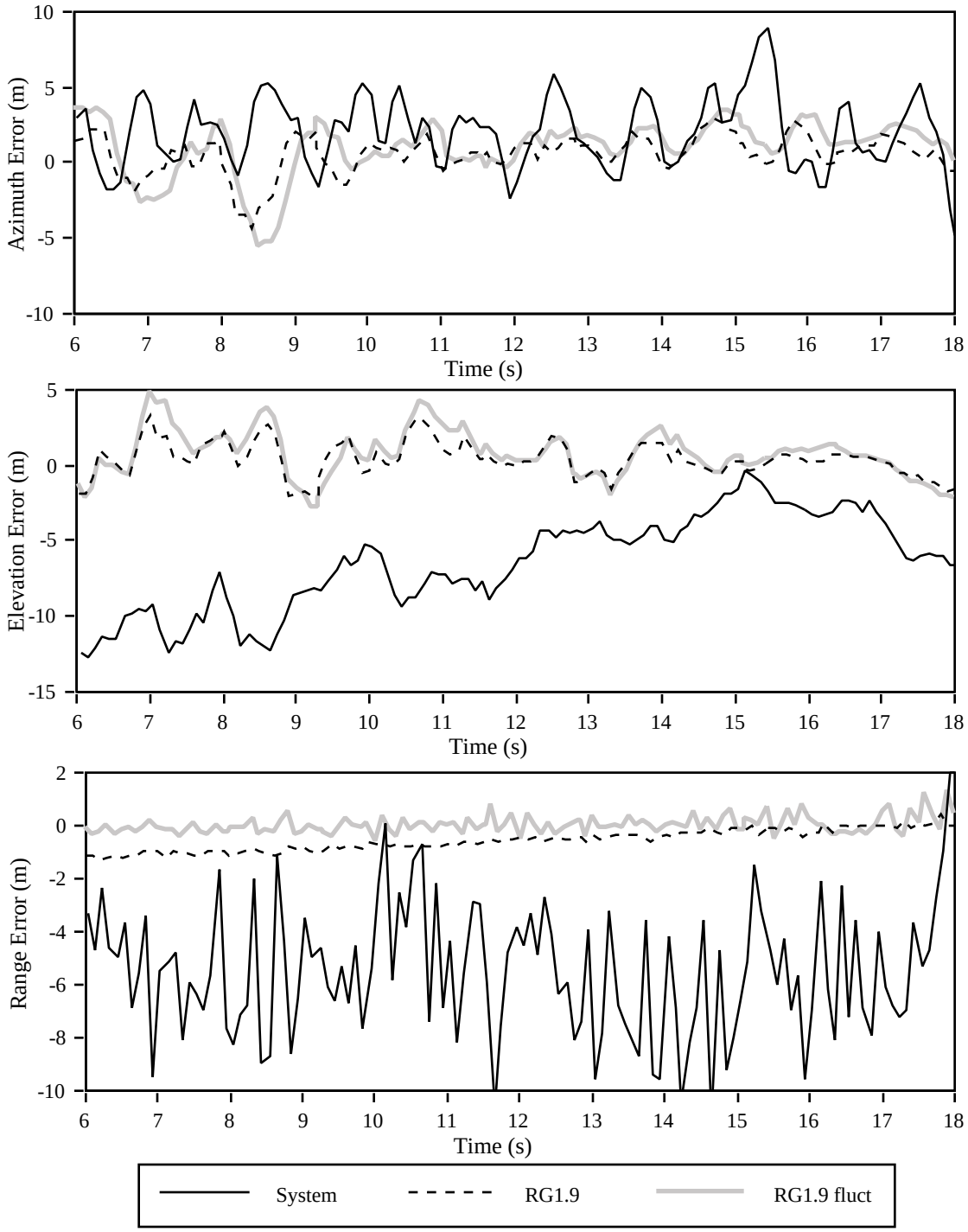

FIGURE 4.2-12. Tracking Errors - T3804146 R04 (6-18 s).

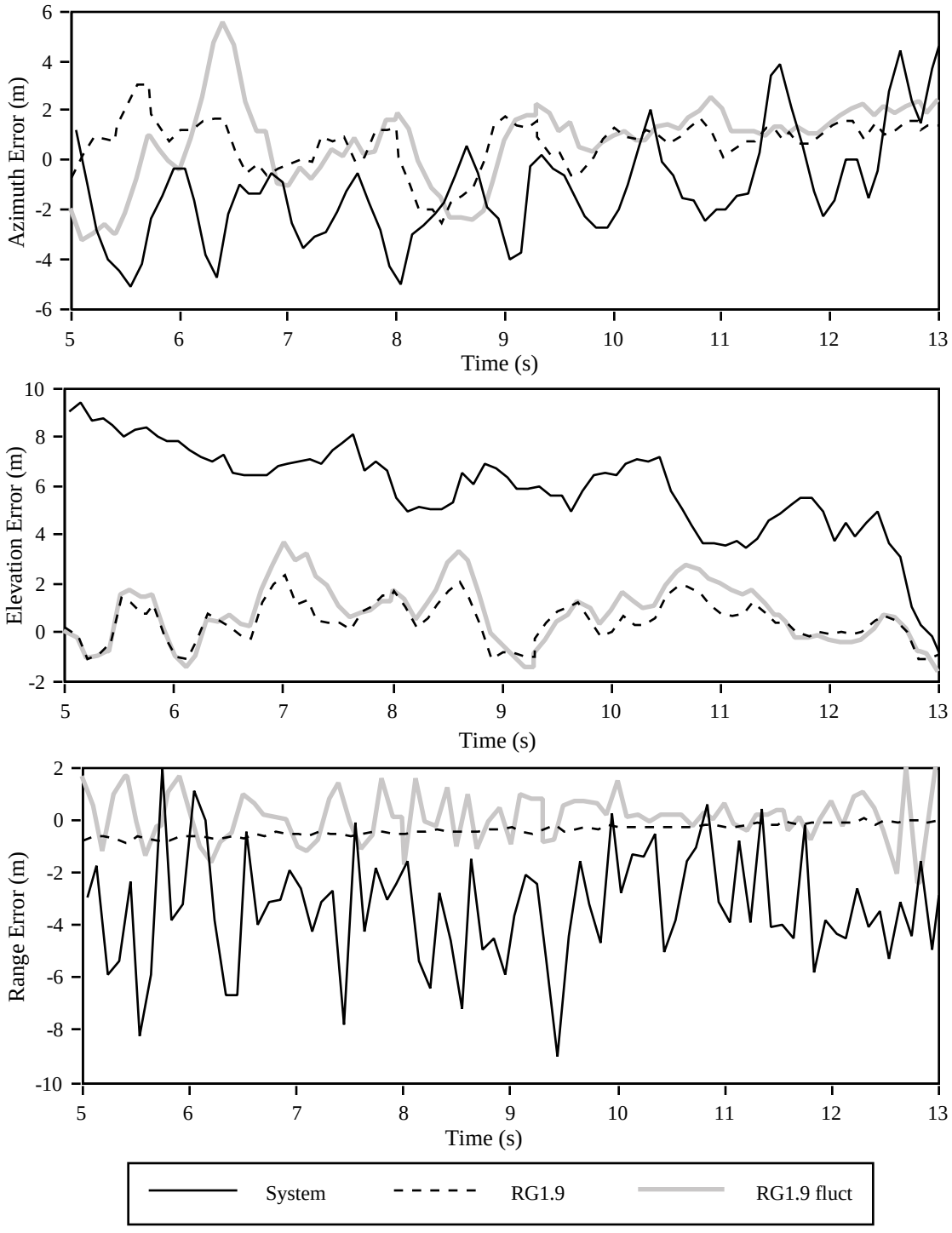

FIGURE 4.2-13. Tracking Errors - T3804146 R07 (5-13 s).

TABLE 4.2-9. Tracking Statistics - T3804146 R04 (6-18 s).

MOE	Azimuth Error (m)			Elevation Error (m)			Range Error (m)		
	SYS	RG1.9	RG1.9 fluct	SYS	RG1.9	RG1.9 fluct	SYS	RG1.9	RG1.9 fluct
$\bar{x}$	2.00	0.52	0.89	-6.54	0.39	0.68	-5.47	-0.57	-0.01
σ	2.41	1.31	1.84	3.16	1.17	1.56	2.53	0.39	0.34
RG	14.96	7.26	9.18	12.28	5.48	7.60	12.4	1.71	1.92
$\lvert\bar{x}\rvert$	2.51	1.12	1.68	6.54	0.95	1.34	5.53	0.58	0.25

TABLE 4.2-10. Tracking Statistics - T3804146 R07 (5-13 s).

MOE	Azimuth Error (m)			Elevation Error (m)			Range Error (m)		
	SYS	RG1.9	RG1.9 fluct	SYS	RG1.9	RG1.9 fluct	SYS	RG1.9	RG1.9 fluct
$\bar{x}$	-1.18	0.67	0.69	5.84	0.43	0.75	-3.32	-0.37	0.15
σ	2.17	1.04	1.71	2.01	0.86	1.26	2.18	0.23	0.94
RG	10.33	5.60	8.86	10.70	3.53	5.39	11.00	1.02	5.25
$\lvert\bar{x}\rvert$	2.04	1.06	1.53	5.87	0.79	1.19	3.43	0.38	0.73

Conclusions - T-38

The effect of adding signature fluctuations is not as apparent as was the case with the B-1B. Again, the errors produced by the model are close to zero with a small standard deviation and range of errors. A constant bias can not be used to bring the system's elevation errors into the range output by the model as they wander in one direction during both time segments. In addition, the elevation errors only fall within the vertical dimension bounds for less than a second in each run. Note, however, that these times (15 seconds in run 4 and 13 seconds in run 7) are the only times where the system and model elevation errors approach each other. Even if the biases in the range channel were removed, neither model run exhibits the standard deviation or range of errors that the system produces.

4.2.3 Assessment – Case 3

Assessment Description - F-16

Test Data Description. Tracking data was collected from a AAA threat against a F-16. This test was conducted on the same range used for B-1B testing, with the same threat. The aircraft flew constant altitude, straight and level profiles at various speeds and offsets from the threat system. The reference trackers used were the same trackers used for the Giant Hawk test, and all data collection and processing techniques used during that test apply here.

TABLE 4.2-11. F-16 Test Matrix.

System	Run	Direction (from/to)	Offset (m)	Offset Direction	Altitude (m)	Speed (m/s)
2	1	SE/NW	1301	SW	1804	173
2	3	SE/NW	1464	SW	1820	174
2	4	NW/SE	401	SW	1807	176
2	10	NW/SE	403	SW	668	177

Validation Methodology. Flight paths and tracking error time histories are presented in Appendix A. Each engagement is labeled with an eight-digit target/threat/date designator and a two-digit run number. Figures 4.2-14 through 4.2-16 show the system tracking error time histories for each run with the horizontal dimension of the target superimposed on the azimuth error plot and the vertical dimension superimposed on the elevation plot. The scale on the range error plot is approximately the length of the aircraft.

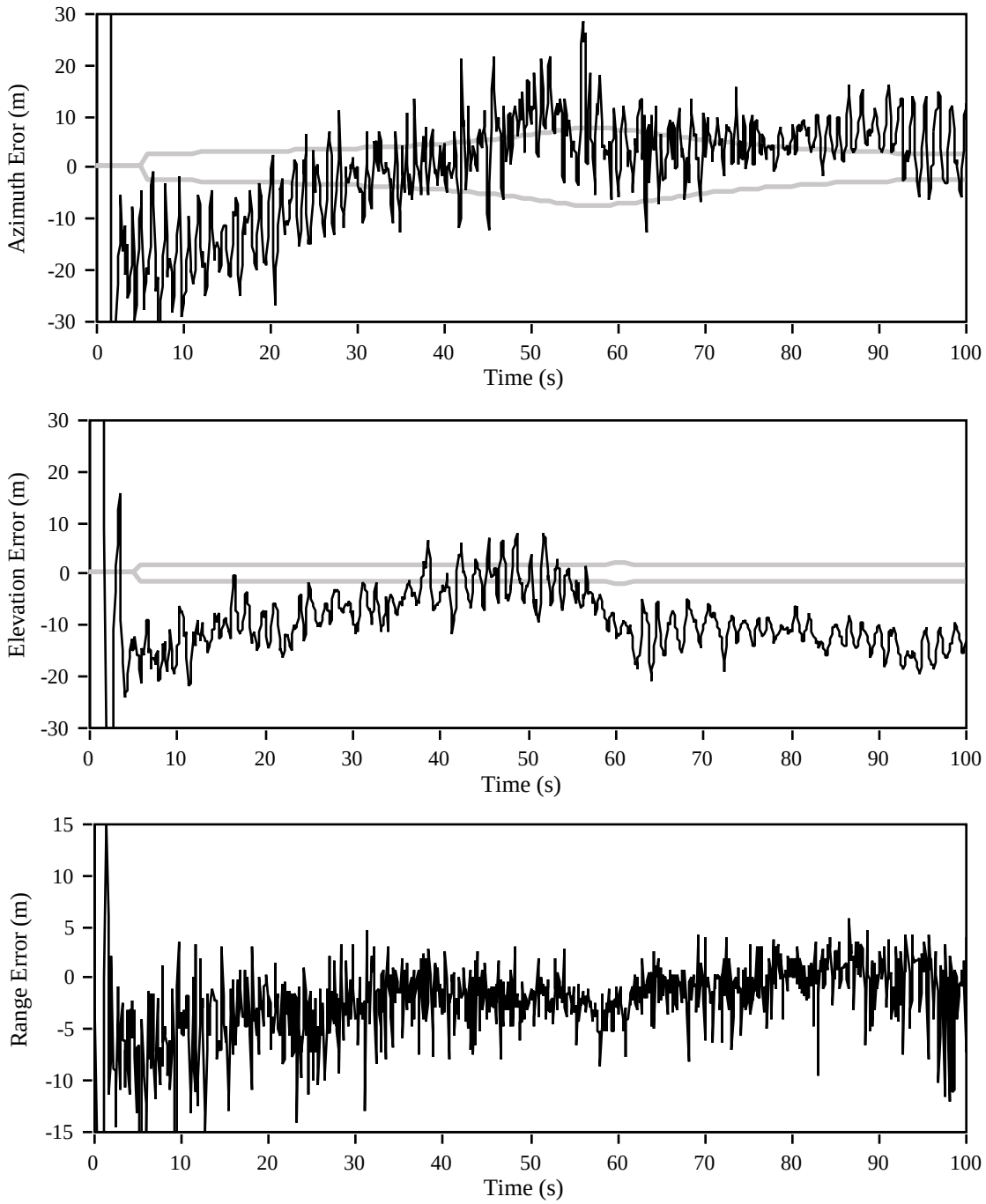

FIGURE 4.2-14. F1602104 R01 (System Tracking Errors).

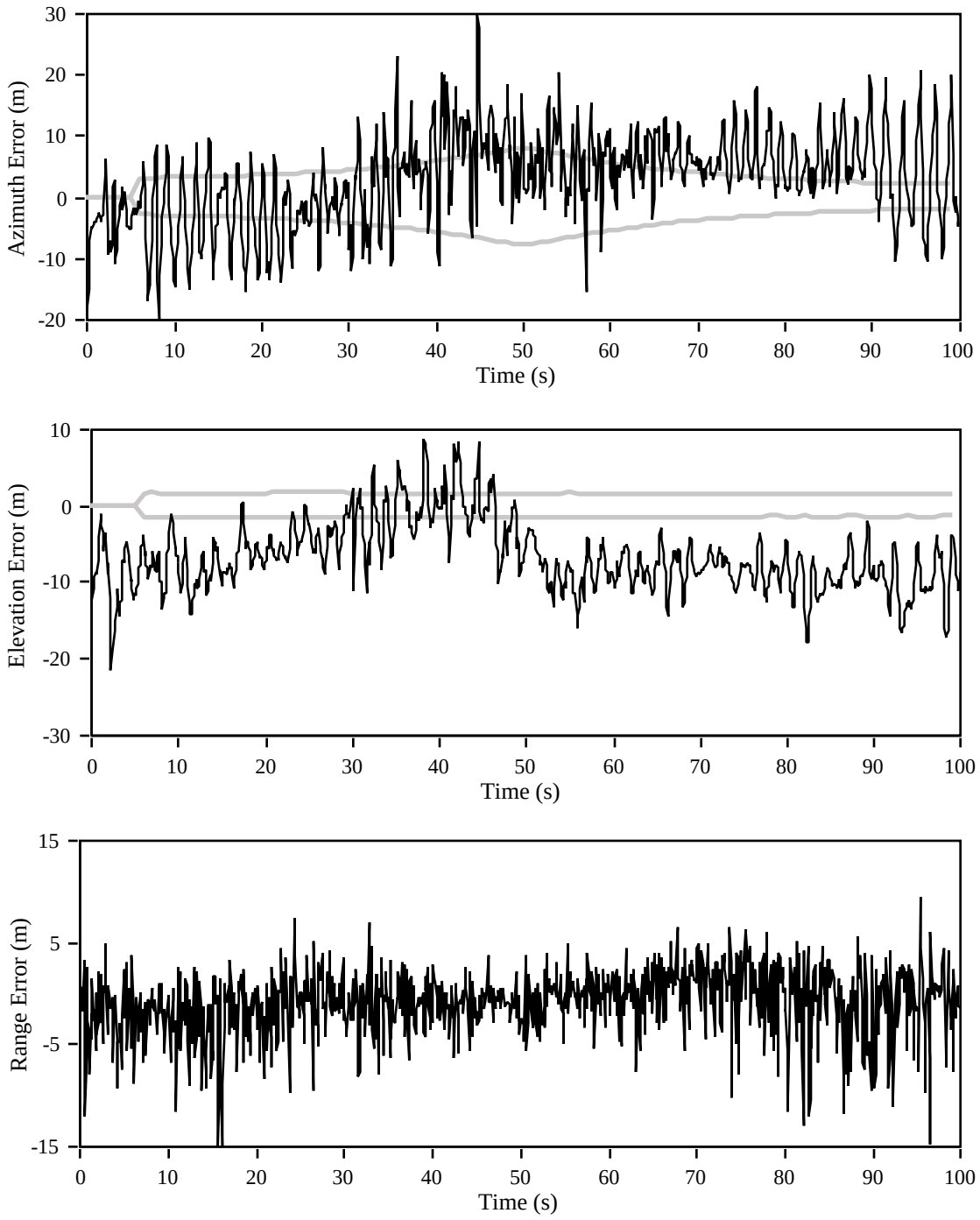

FIGURE 4.2-15. F1602104 R03 (System Tracking Errors).

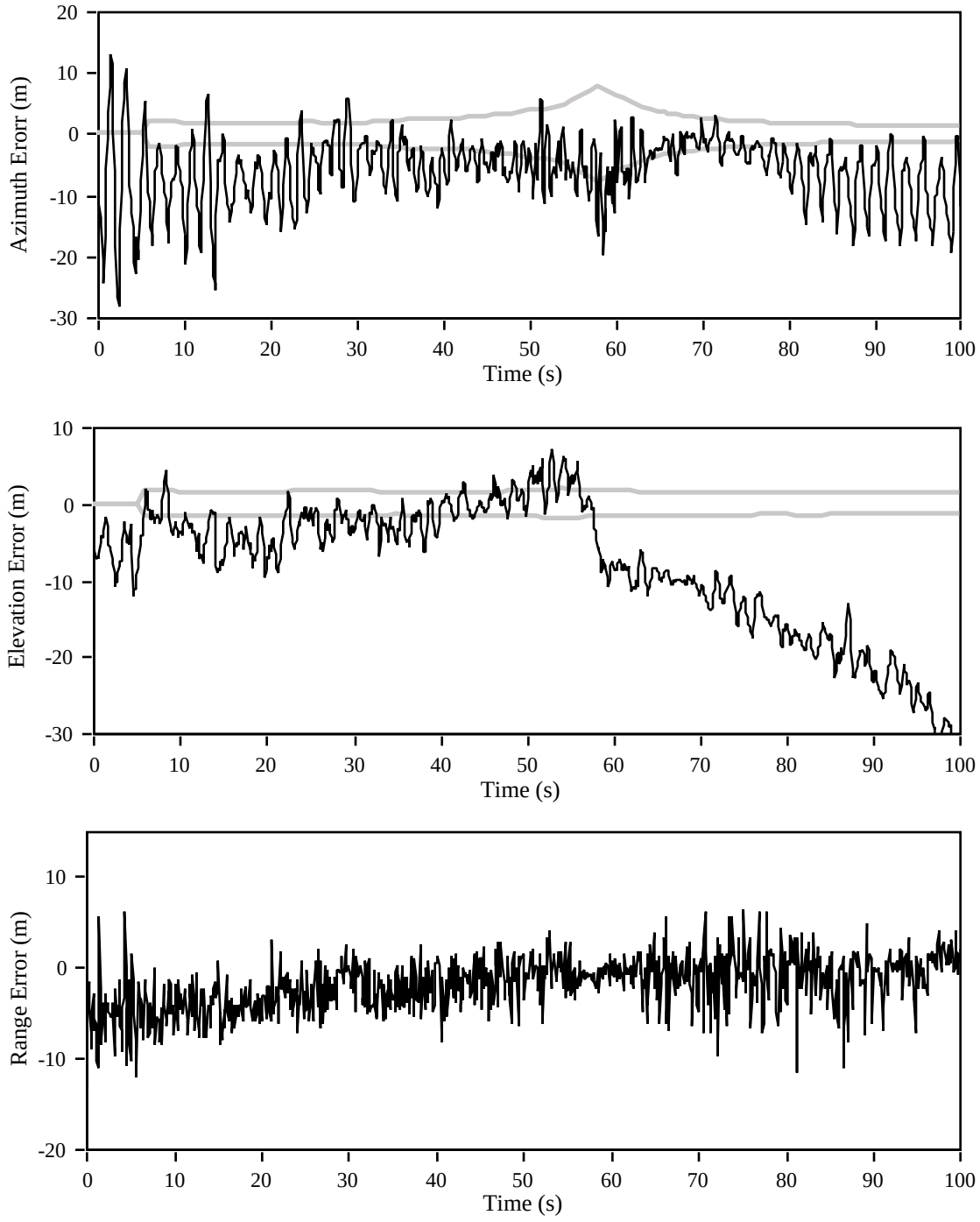

FIGURE 4.2-16. F1602104 R10 (System Tracking Errors.

Results - F-16

During run 1, both the azimuth and elevation errors can be moved into the target dimension bounds by removing constant biases. The elevation errors in run 3 are closest to the dimension bounds from 30 to 40 s. Figures 4.2-17 and 4.2-18 show tracking errors for these

segments. Following the figures are tables containing the mean ($\bar{x}$), standard deviation (s), range (RG), and average of magnitude ($\overline{|x|}$) of errors for each segment. Shaded blocks indicate whether *RADGUNS* v.1.9 with or without target fluctuations best represents the measured MOE.

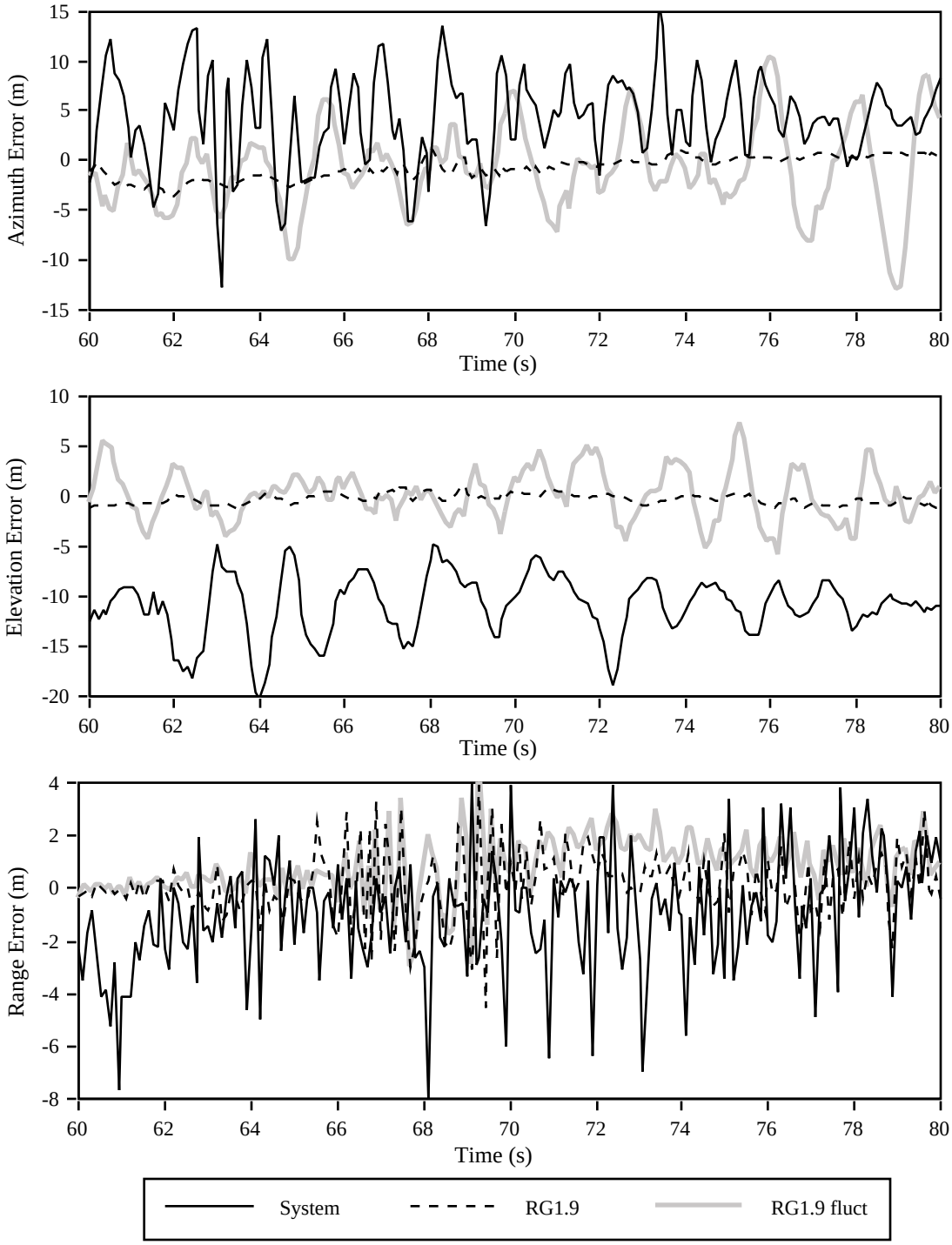

FIGURE 4.2-17. Tracking Errors - F1602104 R01 (60 - 80 s).

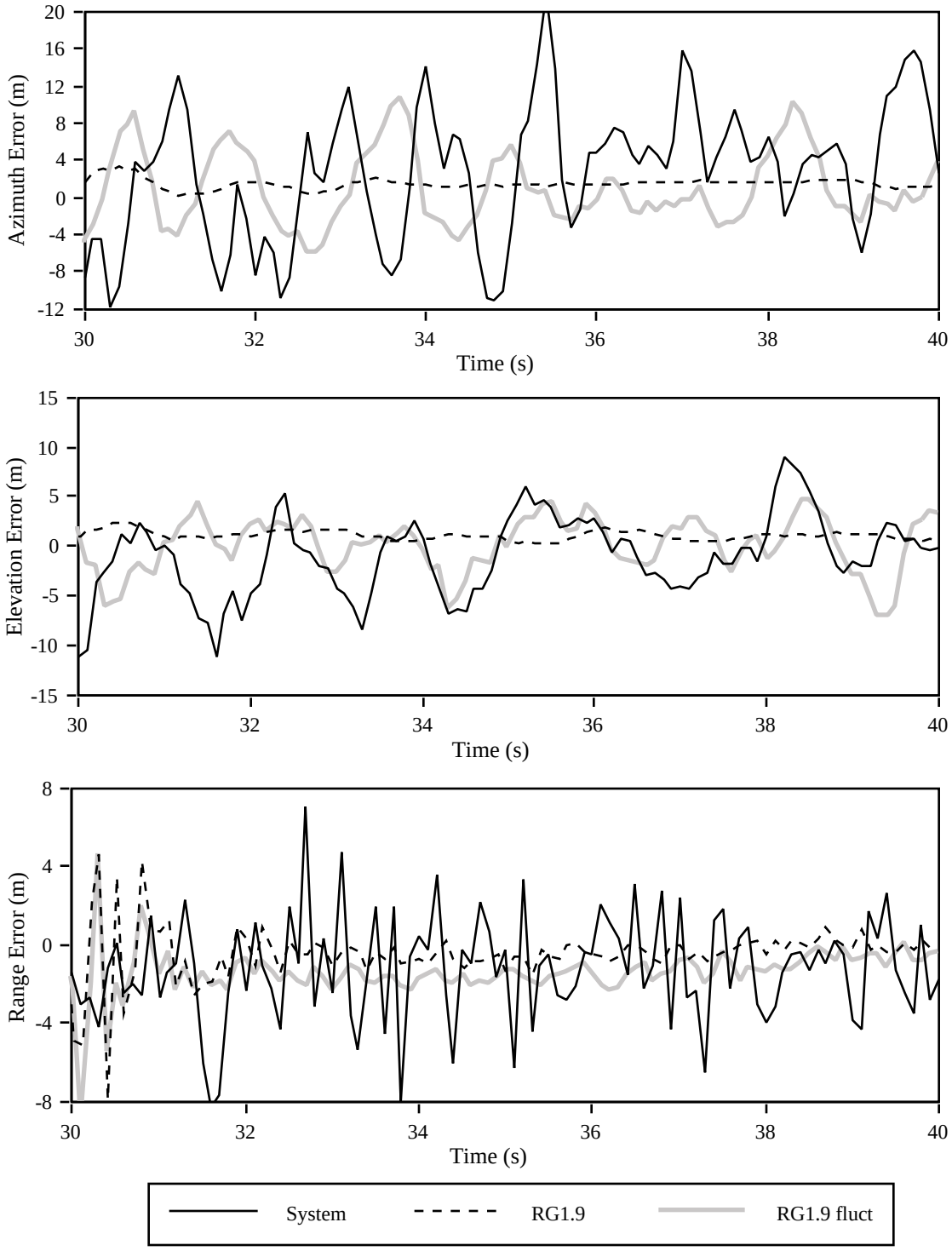

FIGURE 4.2-18. Tracking Errors - F1602104 R03 (30 - 40 s).

TABLE 4.2-12. Tracking Statistics - F1602104 R01 (60 - 80 s).

MOE	Azimuth Error (m)			Elevation Error (m)			Range Error (m)		
	SYS	RG1.9	RG1.9 fluct	SYS	RG1.9	RG19 fluct	SYS	RG1.9	RG1.9 fluct
$\bar{x}$	3.35	-0.48	-0.69	-10.98	-0.36	0.08	-0.96	0.13	0.80
σ	3.28	0.78	3.56	3.01	0.50	2.49	2.19	1.25	1.09
RG	21.26	3.12	20.74	15.90	2.35	13.35	12.30	8.41	7.09
$\overline{\lvert x \rvert}$	3.99	0.75	2.71	10.98	0.51	1.97	1.81	0.92	1.07

With the biases removed from run 1, the measured average of magnitudes is 2.57 m in azimuth and 2.31 m in elevation.

TABLE 4.2-13. Tracking Statistics - F1602104 R03 (30 - 40 s).

MOE	Azimuth Error (m)			Elevation Error (m)			Range Error (m)		
	SYS	RG1.9	RG1.9 fluct	SYS	RG1.9	RG19 fluct	SYS	RG1.9	RG1.9 fluct
$\bar{x}$	2.28	1.23	0.71	-1.03	1.07	0.01	-1.24	-0.44	-1.41
σ	6.29	0.50	3.51	4.01	0.48	2.80	2.72	1.48	1.25
RG	30.72	2.77	14.60	20.14	2.24	11.82	15.20	12.52	13.23
$\overline{\lvert x \rvert}$	5.64	1.23	2.79	3.18	1.07	2.26	2.35	0.91	1.54

Histograms of each segment are shown in Figures 4.2-19 and 4.2-20.

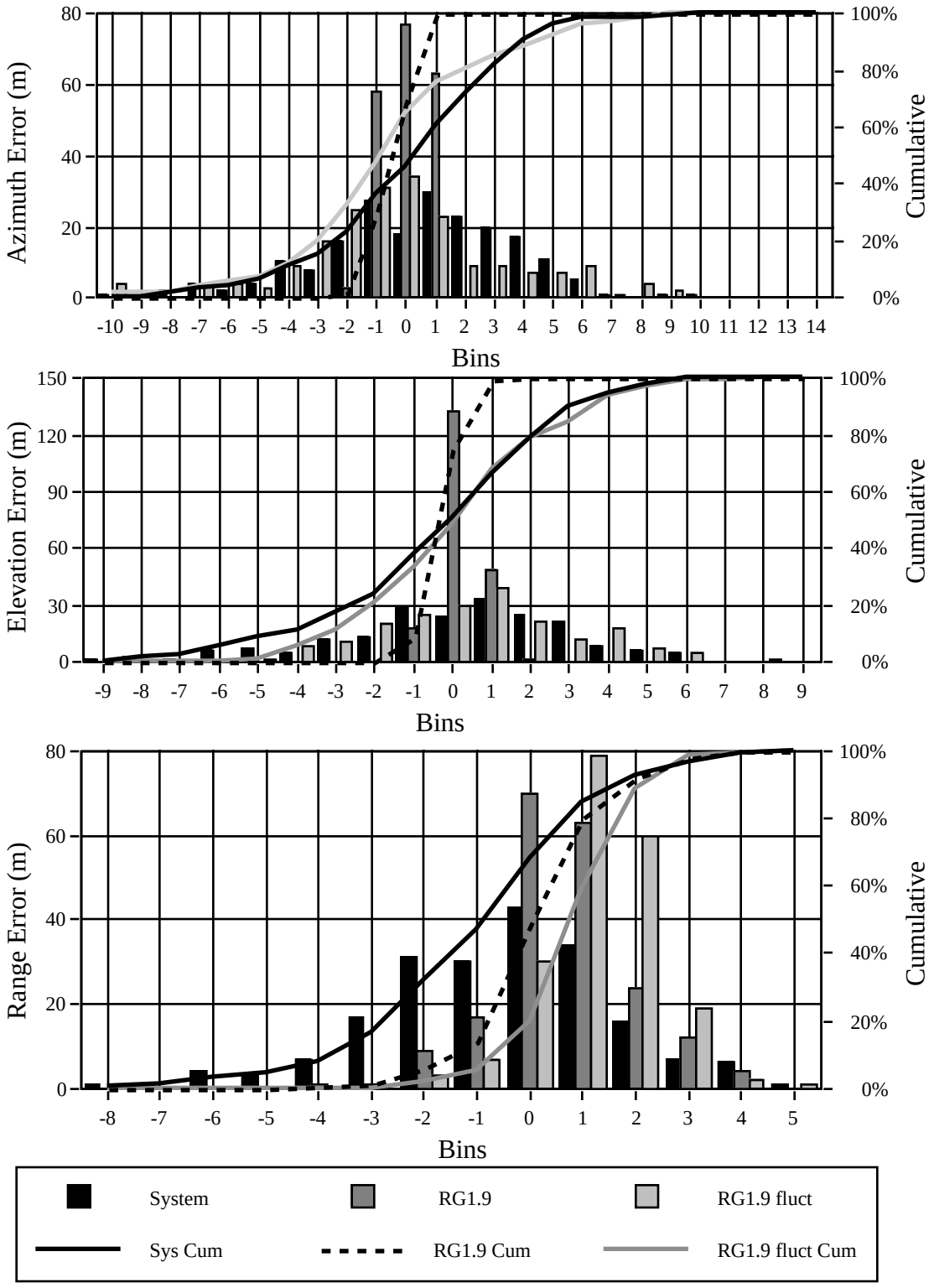

FIGURE 4.2-19. Tracking Error Distribution - F1602104 R01 (60 - 80 s).

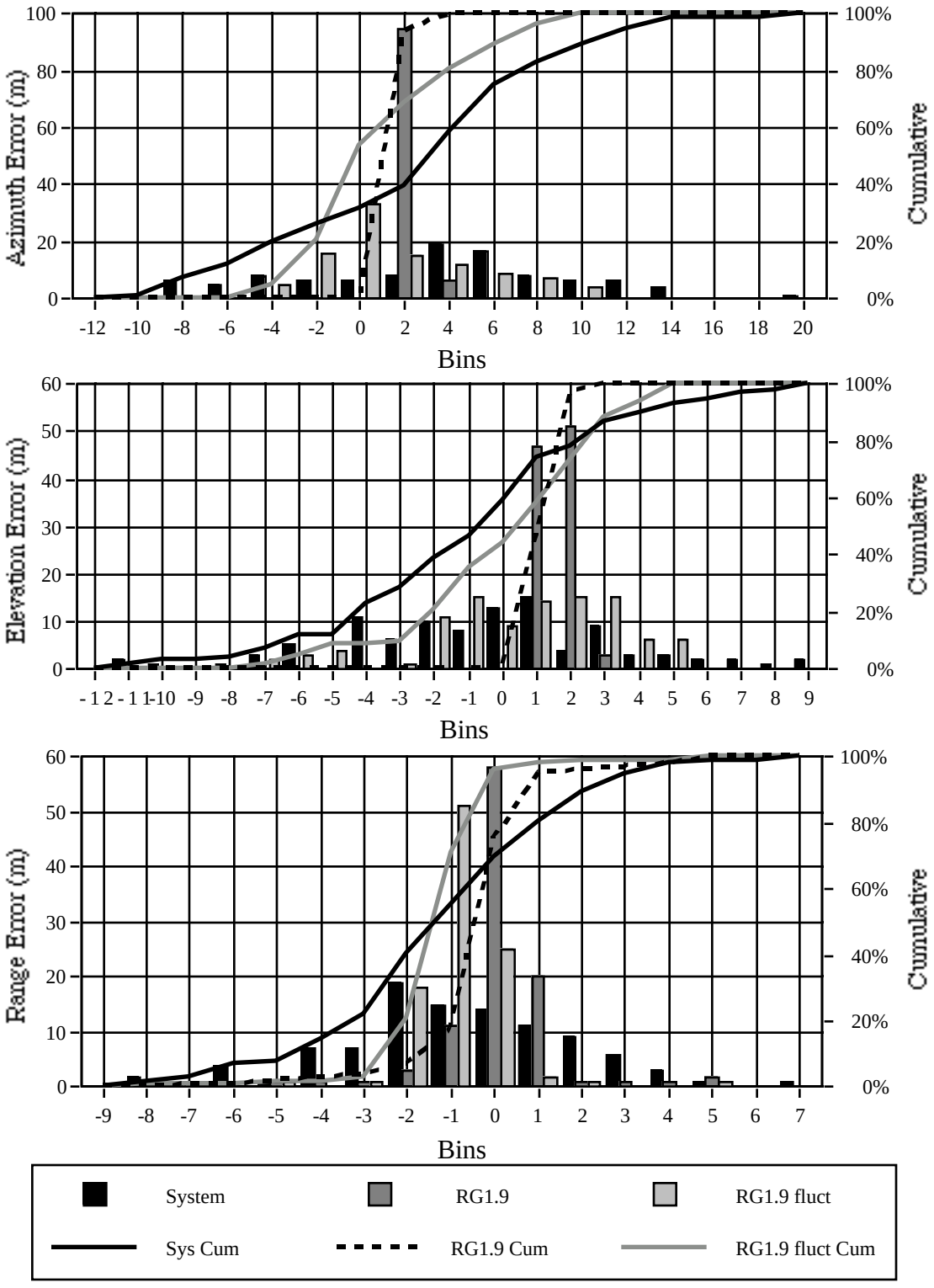

FIGURE 4.2-20. Tracking Error Distribution - F1602104 R03 (30 - 40 s).

Conclusions - F-16

Fluctuating the target signature significantly improves model correlation with test data in both azimuth and elevation. Range errors, however, are not significantly impacted by varying the target signature, and neither model output reflects the magnitude or range of errors produced by the system. Measured range errors are, in general, quite small and the accuracy of these measurements may be limited by the capabilities of the range test equipment used to gather them.

Assessment Description - F-15

Test Data Description. During August of 1993 the West XI-C threat system was realigned as part of its required annual recertification process. Several flight tests with and without ECM were conducted to dynamically evaluate the resulting threat performance. No ECM was used on Day 309 and only passes from that day will be presented here.

Validation Methodology. Prior to delivery, the raw TSPI was first corrected for bias and timing errors, smoothed using a 51-point curve fitting routine, and then translated and rotated to the threat's coordinates. Range documentation lists the TSPI accuracy to 30 feet (9.14 m) in range and 0.3 mrad in angle (0.3 m at a range of 1 km, 1.5 m at 5 km). All data were sampled at 10 Hz. Table 4.2-14 lists the data fields used in this analysis.

TABLE 4.2-14. West XI-C Data Fields.

Field Name	Description
ac x comp	x-component of test A/C from threat
ac y comp	y-component of test A/C from threat
ac z comp	z-component of test A/C from threat
heading	A/C heading
pitch	A/C pitch
roll	A/C roll
delta az	Azimuth error (Threat - TSPI)
delta el	Elevation error (Threat - TSPI)
delta range	Range error (Threat - TSPI)
aux stat 1	Auxiliary status word 1
aux stat 2	Auxiliary status word 2

The status words were used to determine the threat track mode and position of the MTI switch. Table 4.2-15 lists the aircraft's direction of travel, offset, offset direction, altitude, and speed.

TABLE 4.2-15. F-15 Test Matrix.

System	Run	Direction (from/to)	Offset (m)	Offset Direction	Altitude (m)	Speed (m/s)
3	7	S/N	760	E	324	241
3	16	S/N	683	E	637	179

Flight paths and tracking error time histories are presented in Appendix A. Each engagement is labeled with an eight-digit target/threat/date designator and a two-digit run number. Figures 4.2-21 and 4.2-22 show the system tracking error time histories for each run with the horizontal dimension of the target superimposed on the azimuth error plot and the vertical dimension superimposed on the elevation plot. The scale on the range error plot is approximately the length of the aircraft.

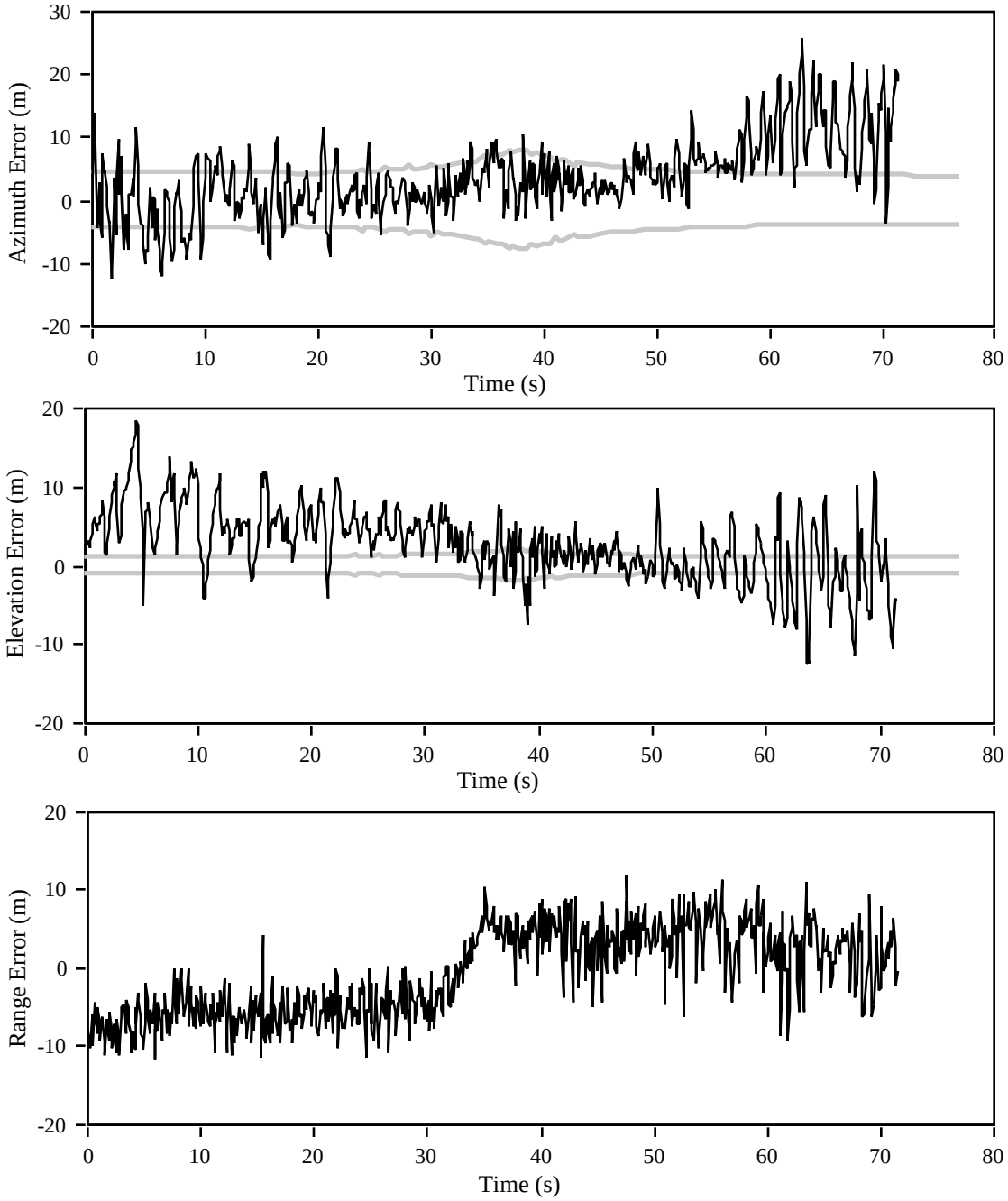

FIGURE 4.2-21. F1503309 R07 (System Tracking Errors).

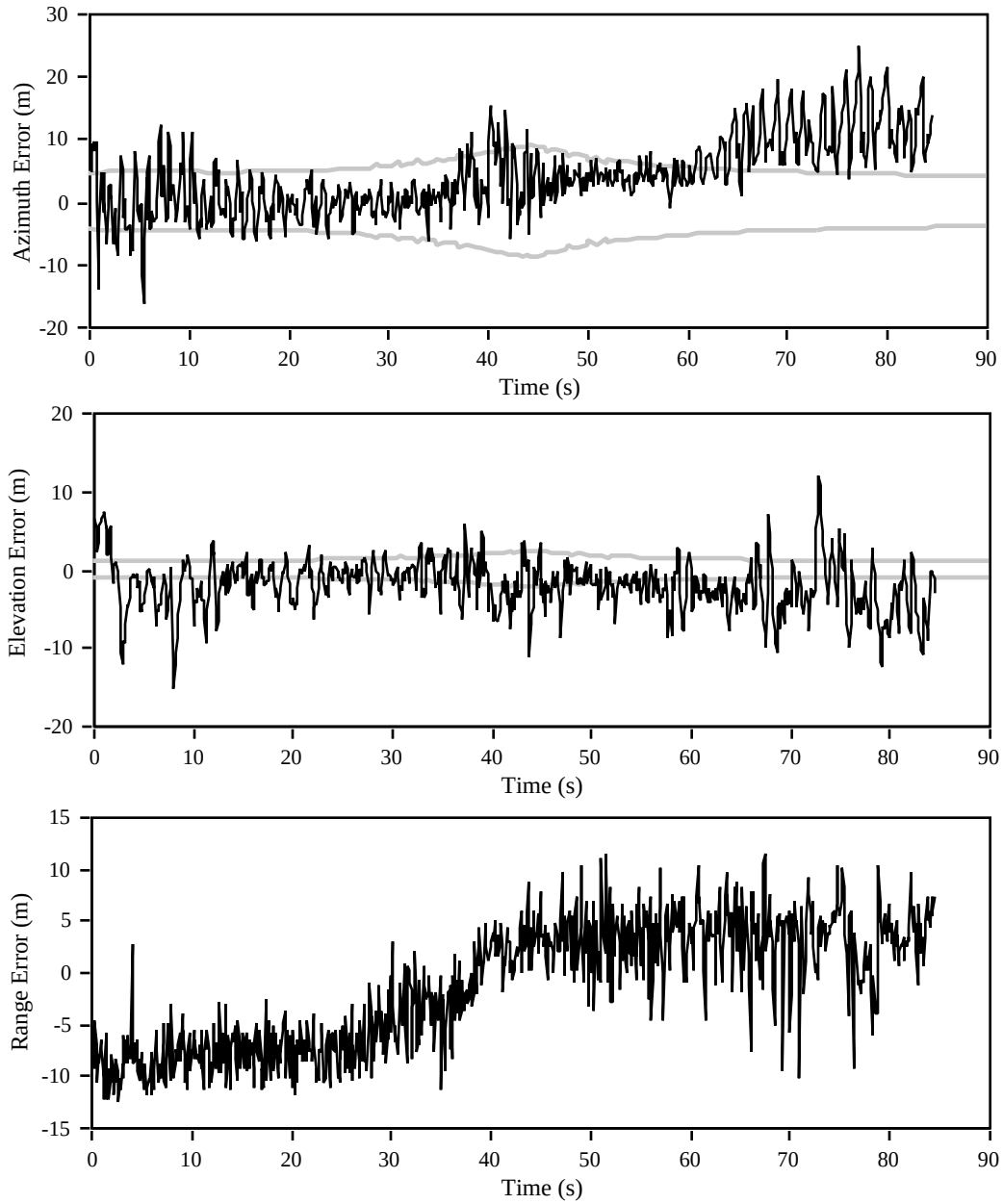

FIGURE 4.2-22. F1503309 R16 (System Tracking Errors).

Results - F-15

Appendix A shows tracking errors measured from the system (labeled System), produced by *RADGUNS* v.1.9 (labeled RG1.9), and produced by *RADGUNS* v.1.9 with a fluctuating RCS (labeled RG1.9 fluct). Angle errors are shown in both mrad and meters. Figures 4.2-23 through 4.2-26 show tracking errors for the portions of passes 7 and 16 where both the azimuth and elevation errors fall reasonably within the target dimension bounds. Following the figures are tables containing the mean ($\bar{x}$), standard deviation (s), range (RG), and average of magnitude ($\overline{|x|}$) of errors for each segment. Shaded blocks indicate whether *RADGUNS* v.1.9 with or without target fluctuations best represents the measured MOE.

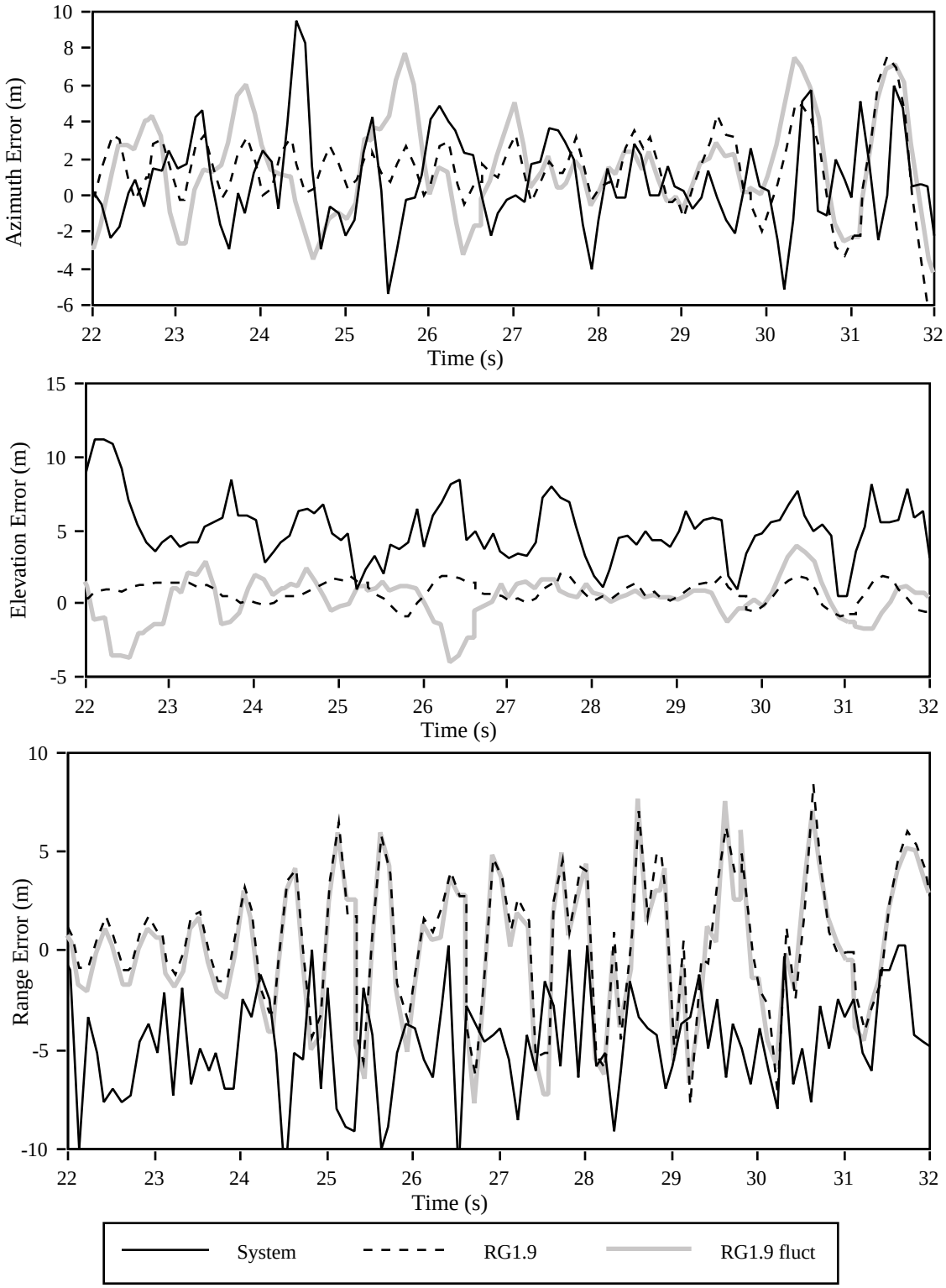

FIGURE 4.2-23. Tracking Errors - F1503309 R07 (22-32 s).

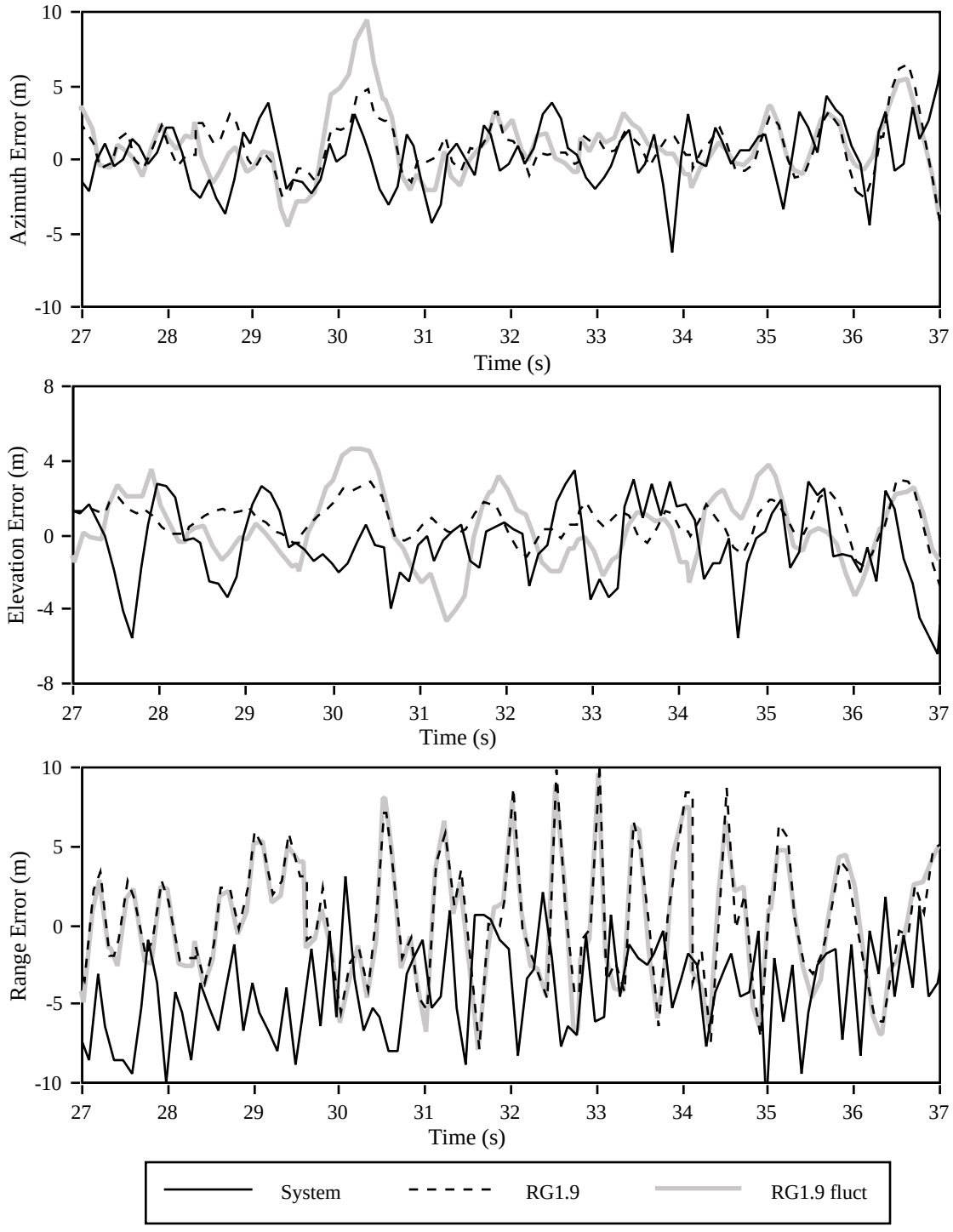

FIGURE 4.2-24. Tracking Errors - F1503309 R16 (27-37 s).

TABLE 4.2-16. Tracking Statistics - F1503309 R07 (22-32 s).

MOE	Azimuth Error (m)			Elevation Error (m)			Range Error (m)		
	SYS	**RG1.9**	**RG1.9 fluct**	**SYS**	**RG1.9**	**RG1.9 fluct**	**SYS**	**RG1.9**	**RG1.9 fluct**
$\bar{x}$	0.59	1.51	0.63	5.30	0.87	0.17	-5.56	0.61	-0.10
σ	4.26	1.23	3.19	3.26	0.54	2.40	2.50	2.56	2.83
RG	20.93	5.42	14.91	16.20	2.90	12.15	15.55	12.76	13.66
$\overline{\lvert x \rvert}$	3.27	1.59	2.72	5.52	0.91	1.89	5.64	2.16	2.22

When the elevation errors are adjusted by a constant bias of 5.27 m, the average of magnitudes becomes 2.49 m in elevation.

TABLE 4.2-17. Tracking Statistics - F1503309 R16 (27-37 s).

MOE	Azimuth Error (m)			Elevation Error (m)			Range Error (m)		
	SYS	**RG1.9**	**RG1.9 fluct**	**SYS**	**RG1.9**	**RG1.9 fluct**	**SYS**	**RG1.9**	**RG1.9 fluct**
$\bar{x}$	-0.30	0.92	0.82	-1.15	0.86	-0.01	-7.58	0.45	0.03
σ	2.60	1.33	3.34	1.87	0.71	1.95	2.13	3.55	3.78
RG	11.02	7.12	15.62	9.49	4.06	9.31	9.45	17.94	17.60
$\overline{\lvert x \rvert}$	2.15	1.25	2.58	1.64	0.93	1.54	7.58	2.93	3.12

Histograms of each segment are shown in Figures 4.2-25 and 4.2-26.

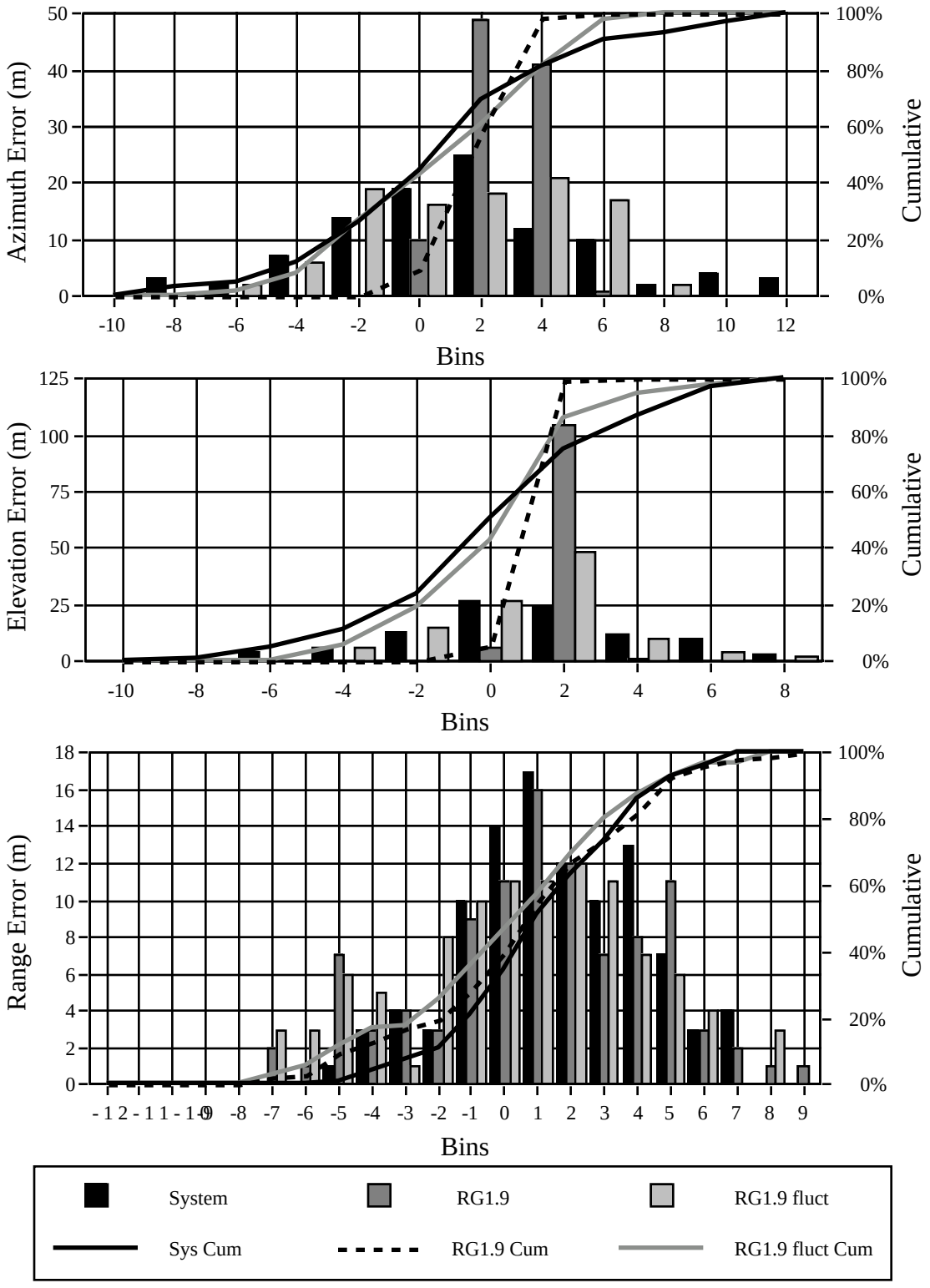

FIGURE 4.2-25. Tracking Error Distribution - F1503309 R07 (22-32 s).

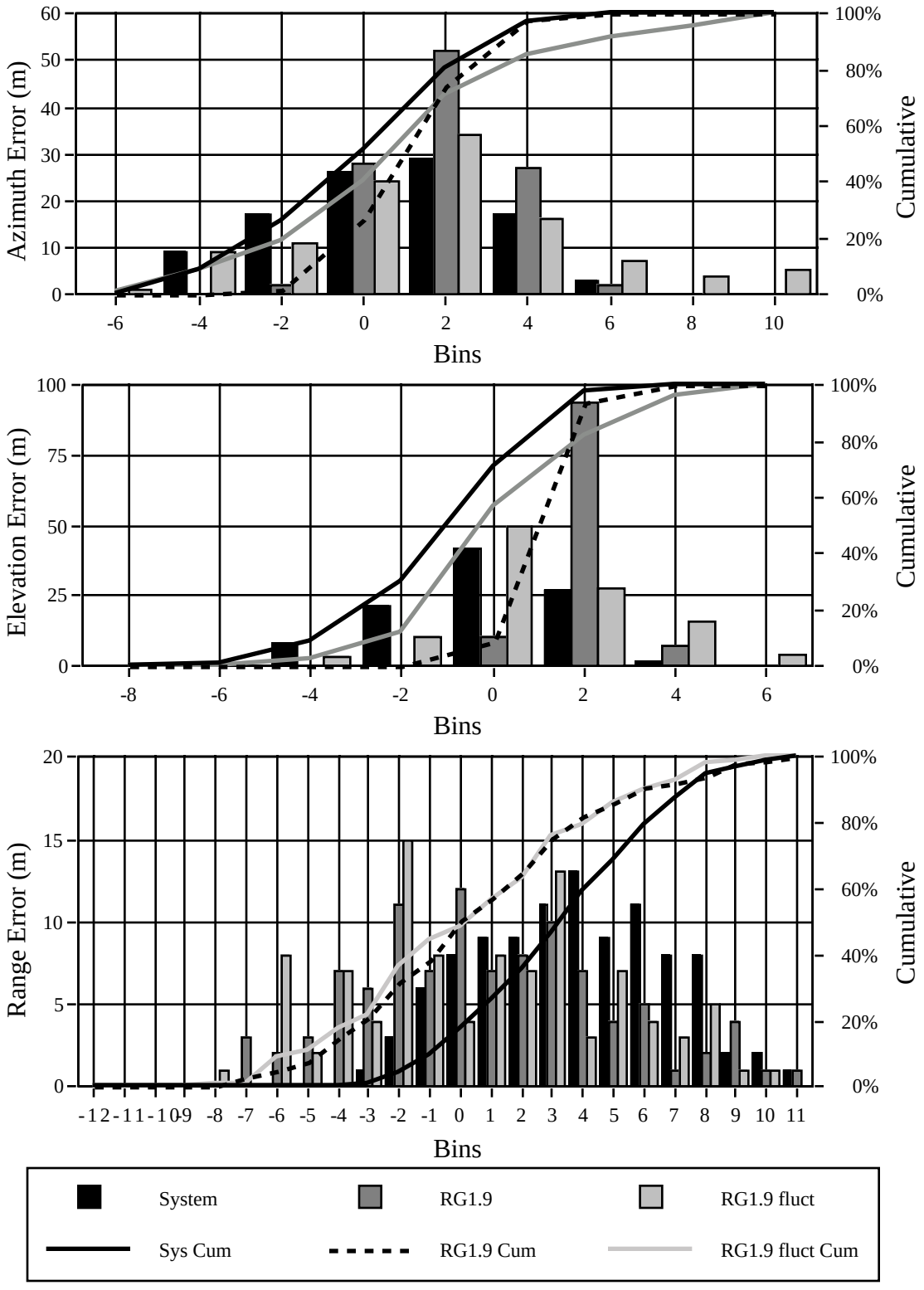

FIGURE 4.2-26. Tracking Error Distribution - F1503309 R16 (27-37 s).

Conclusions - F-15

As with the other targets, fluctuating the signature significantly improves model correlation with test data in both azimuth and elevation. Again, range errors are not significantly impacted by varying the target signature. Correlation with measured range errors, however, is better for this particular target.